

Estimating the Unobservable Components of Electricity Demand Response with Inverse Optimization

Adrian Esteban-Perez

Department of Technology and Operations Management, Rotterdam School of Management, Erasmus University, Rotterdam 3062 PA, The Netherlands estebanperez@rsm.nl

Derek Bunn

London Business School, London NW1 4SA, United Kingdom dbunn@london.edu

Yashar Ghiassi-Farrokhfal

Department of Technology and Operations Management, Rotterdam School of Management, Erasmus University, Rotterdam 3062 PA, The Netherlands y.ghiassi@rsm.nl

Abstract: Understanding and predicting the electricity demand responses to prices are critical activities for system operators, retailers, and regulators. While conventional machine learning and time series analyses have been adequate for the routine demand patterns that have adapted only slowly over many years, the emergence of active consumers with flexible assets such as solar-plus-storage systems, and electric vehicles, introduces new challenges. These active consumers exhibit more complex consumption patterns, the drivers of which are often unobservable to the retailers and system operators. In practice, system operators and retailers can only monitor the net demand (metered at grid connection points), which reflects the overall energy consumption or production exchanged with the grid. As a result, all "behind-the-meter" activities—such as the use of flexibility—remain hidden from these entities. Such behind-the-meter behavior may be controlled by third party agents or incentivized by tariffs; in either case, the retailer's revenue and the system loads would be impacted by these activities behind the meter, but their details can only be inferred. We define the main components of net demand, as baseload, flexible, and self-generation, each having nonlinear responses to market price signals. As flexible demand response and self generation are increasing, this raises a pressing question of whether existing methods still perform well and, if not, whether there is an alternative way to understand and project the unobserved components of behavior. In response to this practical challenge, we evaluate the potential of a data-driven inverse optimization (IO) methodology. This approach characterizes decomposed consumption patterns without requiring direct observation of behind-the-meter behavior or device-level metering. By analyzing net demand as revealed at the grid connection point, we estimate parameters for a latent optimization model, enabling predictions that infer the unobservable components. We validate the approach using real-world data, demonstrating its superior performance in both point and probabilistic forecasting compared to state-of-the-art time-series analysis and machine learning benchmarks.

Key words: Unobservable Behavior, Electricity, Forecasting, Behind-the-Meter, Inverse Optimization, Demand Forecasting

1 Introduction

Understanding and predicting the electricity demand responses to prices are critical activities for system operators (SO), retailers and regulators. For system operators, accurate demand forecasts are essential to

ensure that energy supply meets demand within the grid's capacity limits and other physical constraints (Shahidehpour et al. 2002). For electricity retailers, these predictions are vital for revenue management, cost control, and tariff design to provide better pricing for consumers (Karthikeyan et al. 2013), whilst for regulators and policy-makers, promoting efficient consumer engagement has become an important element in their net zero ambitions (Pinson et al. 2014).

Electricity demand forecasting at the consumer level has been widely researched and, in practice, had until recently reached acceptable levels of accuracy, largely due to the relatively stable nature of consumer behavior (Hatton et al. 2015). However, recent developments associated with the energy transition have radically altered all elements of the electricity supply and value chain. These changes have been driven by substantial subsidies for decarbonization and the emergence of end-user generation. As a result, system operators have recognized an urgent need for energy *flexibility* to help balance supply and demand (Pinson et al. 2014). Flexibility in this context mainly refers to the ability to adapt energy consumption patterns, such as shedding demand during periods of high energy prices or grid stress, or shifting demand to times when energy is cheaper or the grid is less stressed. To promote consumer flexibility, retailers have introduced new incentive mechanisms, including Time-of-Use (TOU) pricing and dynamic pricing models, which align flexibility with grid status and/or temporal energy prices (Vardakas et al. 2014). In response, cost-conscious consumers have increasingly embraced flexibility e.g., by adopting solar-plus-storage systems and opportunistically scheduling their electric vehicle charging, thereby enhancing their ability to manage energy costs and contribute to grid stability (Danti and Magnani 2017).

As a result of these changes, accurate estimation of the consumer demand response in the evolving retail electricity markets has become both more critical and more complex. This importance has increased because energy procurement is now more challenging due to the added volume and uncertainty, pushing the traditional grid closer to its limits and raising the risk of congestion (Koliou et al. 2015). The complexity has grown because, unlike in the past where demand was generally non-price responsive with a stable profile over time, today's consumer demand, as observed by SOs and retailers at the metering point with the grid, is confounded by new unobservable components. The essential baseload demand (unresponsive to price) is supplemented with price-responsive flexible demand (including batteries and electric vehicles) and reduced by any end-user generation (e.g., solar). Accurately estimating these components would require retailers and SOs to know the types and capacities of flexible devices owned by consumers and to have access to real-time device-level data on how consumers operate these assets to manage costs. However, this information, known as behind-the-meter (BTM) behavior, is typically hidden from SOs and retailers. In fact, not only are they often unaware of the devices owned by consumers—sometimes even including solar panels—but they also may be unable to access or utilize real-time device-level measurements. This data is typically classified as personal information and protected by privacy legislation, for example by the General Data Protection Regulation (GDPR) in the EU (European Parliament and Council 2016), and sometimes by considerations

of cybersecurity in smart systems (Liu et al. 2012). The difficulty and importance of accurately characterizing BTM flexibility behavior has prompted a call to action among practitioners and policymakers. For instance, an IEEE Task Force is now dedicated to the estimation, optimization, and control of BTM behavior (Srivastava et al. 2024).

Consequently, SOs and retailers need to estimate the unobservable behind-the-meter information in the absence of direct measurements. But existing methodologies, such as time-series analysis (Choi et al. 2020, Dong et al. 2017) and machine learning algorithms have generally been applicable only to the observable demand, as metered at the grid connection point (“net demand”) rather than the specific latent components of consumer demand which may be flexing (Nghiem and Jones 2017, Wen et al. 2020). To address this methodology gap, we question if the emerging technique of inverse optimization (IO) could offer a promising solution for estimating the unobserved information on these components, thereby potentially enhancing the prediction of observable net demand. IO operates by modeling a consumer’s behind-the-meter price response as a latent optimization problem under different pricing schemes and then integrating this into an optimal prediction problem. This approach has the potential to capture nonlinear consumer responses by distinguishing between the flexible, inflexible, and self-generation components of demand, thereby improving the specification of the net demand response. Whether this decomposition then leads to improved net demand forecasts is the open research question that we address.

This work is positioned as a contribution from the Green Information Systems (Green-IS) body of research to the net zero electricity transition. Green-IS research advances the vital role of information systems and clean technologies in promoting environmentally sustainable practices (Sunar and Swaminathan 2022), aligned with the principles of eco-efficiency and eco-effectiveness (Loock et al. 2013). Specifically, (Watson et al. 2010, Fig. 1) encourages the Green-IS research themes to include “energy informatics” to help reduce energy consumption and achieve sustainable energy solutions. In this paper, we contribute to this effort by helping retailers and SOs estimate unobservable information in demand behavior.

The key contributions of this paper are therefore summarized as follows:

- **Domain Contributions:** This paper makes a substantial contribution to characterizing the unobserved components of electricity demand response, being, as far as we are aware, the first to do so in the absence of device-level, real-time measurements. We accomplish this by developing an application of inverse optimization (IO) to this critical issue, a method previously used in other fields but not yet in retail electricity. Unlike conventional approaches that depend on direct observations of device-level data, this new method leverages net demand data to estimate unobservable flexibility parameters within a latent optimization model.
- **Experimental Results:** To validate the performance of the proposed methodology, we conduct a two-stage analysis using real-world data from previous studies. In the first stage, we utilize a dataset from Kaggle, which provides access to detailed, device-level, behavior of a US household with the aim of

supporting multiple replication studies. Applying inverse optimization (IO) to this data, we find that the estimated flexible and inflexible components of demand align well with actual device behavior, confirming the plausibility of our approach. However, this dataset lacks Time-of-Use (TOU) pricing. To address this, we proceed to the second stage using a dataset from a study in Japan, which includes TOU prices but lacks observable device behavior. Building on the validation of our IO approach in the first stage, we then compare its fitting and forecasting capabilities on this data against benchmark models. The IO approach not only demonstrates superior empirical performance but also provides explicit estimates of the unobservable flexible and baseload demand components.

- **Managerial Implications:** This methodology allows retailers and system operators to gain a deeper understanding of behind-the-meter flexibility without compromising data privacy or requiring real-time device-level measurements. It can help them forecast better and enhance their incentive mechanisms, resulting in benefits for themselves and consumers through more efficient green energy management.

The rest of the paper is organized as follows. Section 2 reviews the related literature. In Section 3, we introduce the problem. In Section 4, we provide the proposed IO model and its tractable reformulation. Section 5 reports the empirical results and Section 6 concludes the paper.

2 Background research

Two research streams relate to our work. One is about the domain focus and the other is about the methodology. We discuss these two research streams, separately.

2.1 Estimating and predicting behind-the-meter demand

Various attempts to decompose "behind-the-meter" consumer demand into its inflexible baseload and flexible, price responsive, components have ranged from statistical and optimization techniques to machine learning approaches (Dobakhshari and Gupta 2018, Hatton et al. 2015, Lei et al. 2020, Sun et al. 2019, Wen et al. 2020, Zhang et al. 2015). The simplest method of estimating baseload demand using the average demand from periods without flexibility incentives, whilst appealing, has led to significant inaccuracies. More advanced statistical methods using linear or non-linear regression models with explanatory variables have resulted in weakly significant baseload estimates, with higher precision requiring large datasets. Regarding the flexible demand component, whilst its price response is confounded with other behavioral and weather-dependent factors, probabilistic methods including Bayesian inference and machine learning have provided useful insights into these uncertainties (Lin et al. 2021, Vallés et al. 2018, Mahdavi et al. 2022, Zhang et al. 2022). Nevertheless, all these methods encounter significant challenges, particularly in capturing temporal dependencies, handling nonlinear characteristics, and in context generalizations.

A fundamental issue with the regression methods, both statistical and machine learning, is that the training (estimation) relies on regressors rather than being driven by actual end-user's price responses. This has been emphasized by [Chen et al. \(2024\)](#), [Hekmat et al. \(2023\)](#). Moreover, various empirical studies have identified limitations associated with nonlinear effects, delayed responses and a general tendency for over-estimated price responses ([An et al. 2015, 2016](#), [Cappers et al. 2010](#), [Kirschen et al. 2000](#)). The methods prevalent in existing research struggle with these and other limitations, primarily due to rigid assumptions in the elasticity models ([Ruan et al. 2021](#)), the lack of interpretability in machine learning ([Ponoćko and Milanović 2018](#)), and the misalignment between demand baseline estimation and flexibility components ([Vallés et al. 2018](#)). For example, [Ruan et al. \(2021\)](#) introduce Siamese LSTM networks to estimate time-varying elasticities through a two-stage process. Similarly, [Ponoćko and Milanović \(2018\)](#) propose a two-step approach that first decomposes load using device-level data, followed by load forecasting with an artificial neural network. In another study, [Vallés et al. \(2018\)](#) utilize a quantile regression method to capture demand flexibility by incorporating exogenous features such as requests to adjust demand, incentives, ambient temperature, and time of day. However, this approach requires (i) prior knowledge of the demand baseline (often predicted in the absence of price incentives) and (ii) the upward/downward consumer's response, which is typically unobservable. Furthermore, the two-step process—baseline estimation followed by quantile regression-based forecasting—can introduce biases in both net load forecasting and the estimation of baseline demand and flexibility estimates.

In consideration of the limitations in the existing research, an important feature of the IO approach, as developed in this paper, is that it integrates the forecasting and demand decomposition elements endogenously within the overall model, rather than as a sequence of separate tasks. This can thereby capture the complex interactions more robustly to provide more accurate predictions whilst maintaining both interpretability and uncertainty quantification. This appears to be beneficial compared to the conventional approach of modeling the elements separately as a sequence of demand estimation, flexibility quantification, forecasting and uncertainty assessment ([Srivastava et al. 2024](#), Table II).

2.2 Inverse optimization

As its name implies, Inverse Optimization takes the results of a presumed optimization process to infer the parameters in the formulation of the decision-maker's optimal actions. [Chan et al. \(2023\)](#) provide a comprehensive review of its theory and applications. In practice, real data does not usually permit an exact derivation of the parameters, with noise in the observed results being due to measurement errors, bounded rationality, or model miss-specifications. Thus, the IO methodology in this case seeks to minimize the fitting errors between the observed data and the prescribed model results to make them "approximately" optimal ([Aswani et al. 2018](#), [Mohajerin Esfahani et al. 2018](#)). Nevertheless, empirical evidence has shown that where a latent agent optimization model is plausible, the IO approach has greater predictive accuracy

than machine learning and time-series models with limited data (Bian et al. 2023, Fernández-Blanco et al. 2021b, Saez-Gallego and Morales 2017). Power systems have been particularly fertile for the successful applications of IO (Saez-Gallego and Morales 2017).

Related to the demand response context of interest here, Bian et al. (2022, 2023) develop an IO approach using prior model knowledge and a gradient descent algorithm to determine the best-fitting model parameters based on the historical price and response data for forecasting price-responsive behaviors. Shi and Xu (2023) consider a deep learning method embedded into a bi-level model and solved by a gradient-descent method. The research by Fernández-Blanco et al. (2021a,b), Saez-Gallego et al. (2016), Saez-Gallego and Morales (2017) proposes a data-driven IO model for forecasting purposes by reducing the inherent bi-level optimization in these applications to a single-level one. Then, by relaxing the complementary slackness conditions due to the computational hardness, they solved the problem by employing a heuristic method. Kovács (2021) apply IO to extract parameters from electricity consumer models by a quadratically constrained quadratic program which was solved using successive linear programming (SLP), but expressed concerns about the convergence properties of the SLP approach.

We extend this body of work methodologically by developing a computationally efficient reformulation of the IO program to solve a conic mixed integer program. To our knowledge, this is the first study that simultaneously provides accurate demand forecasting as well as a decomposition into its unobservable components, without using direct device measurements. The proposed reformulation relies on the underlying conic-based structure, binary variables (to model the intrinsic combinatorial nature of load shifting) and kernel regression techniques, as advocated by Fernández-Blanco et al. (2021b), to minimize the out-of-sample forecasting errors. We avoid the need to apply a gradient descent method (Bian et al. 2022, 2023) being aware, in particular, that gradient-based algorithms have problems handling bi-level formulations with binary variables (Zhou et al. 2024). We also avoid the need to relax the complementary slackness conditions and apply a heuristic, as used by Fernández-Blanco et al. (2021a,b), Saez-Gallego et al. (2016), Saez-Gallego and Morales (2017).

Thus, the contribution of this work is to develop and apply a novel IO formulation that (i) uses net demand data to estimate for the first time the unobservable load components in an interpretable way and (ii) specifies the demand-response behavior of the consumers with a set of predictive functions to better understand potential flexibilities. Our proposed method is also able to provide the shiftability and sheddability estimates going beyond the approaches proposed elsewhere (Chen et al. 2024, Hekmat et al. 2023).

3 Model

In this section, we present the model. Throughout the paper, bold lower-case letters denote vectors, while standard lower-case letters are reserved for scalars. We use the shorthand $[T] = \{1, \dots, T\}$ to represent the set of all integers up to T . For reference, we also include all notations in Table 1.

Notation	Abbreviations
SO	System operator
TOU	Time-Of-Use
IO	Inverse optimization
FOP	Forward optimization program
BTM	Behind-the-meter
IS	Information Systems
GDPR	General Data Protection Regulation
SLP	Successive Linear Programming
Notation	Indices and Sets
$[T]$	Review period set, defined as $[T] = \{1, \dots, T\}$ made by T hours
t	Index of time period (hours) ($t \in [T]$)
$[S]$	Set of S days defined as $[S] = \{1, \dots, S\}$
s	Index of the daily samples ($s \in [S]$)
Θ	Flexibility feasibility set
Notation	Exogenous variables and parameters
$\hat{\mathbf{d}}_s$	Vector T -dimensional of load measurements on day s (kWh)
\mathbf{g}_s	Vector of T -dimensional renewable energy generation on day s (kWh)
p_t	Price/flat tariff at time t (c/kWh, JPY/kWh)
$p_{s,t}^{sf,+}$	Per unit price incentive of energy of shifting by increasing at time t on day s (c/kWh, JPY/kWh)
$p_{s,t}^{sf,-}$	Per unit price incentive of energy of shifting by decreasing at time t on day s (c/kWh, JPY/kWh)
$p_{s,t}^{sd}$	Per unit price incentive of energy of shedding at time t on day s (c/kWh, JPY/kWh)
\mathbf{z}_s	Vector of T -dimensional exogenous observations build up by price on day s
$\hat{\boldsymbol{\xi}}_{s,t}$	Vector of external features at time t on day s (kWh)
α	Forgetting factor parameter
ω_t	Normalized forgetting weight on day s
$c_{s,t}^{sd}$	Comfort cost incurred by load shedding at time t on day s (c/kWh ² , JPY/kWh ²)
$c_{s,t}^{sf,+}$	Comfort cost incurred by load shifting by increasing demand at time t on day s (c/kWh ² , JPY/kWh ²)
$c_{s,t}^{sf,-}$	Comfort cost incurred by load shifting by decreasing demand at time t on day s (c/kWh ² , JPY/kWh ²)
\mathbf{c}_s	Vector of T -dimensional exogenous observations build up by cost on day s
\mathbf{K}_t	Vector of physical upper bounds of the flexibility envelopes at time t defined by $(K_t^{sf,+}, K_t^{sf,-}, K_t^{sd})$ (kWh)
T^{\max}	Maximum number of shifted hours
ℓ	Utility function
Notation	Endogenous variables
d_t^{bl}	Baseload demand at time t (kWh)
$d_{s,t}^{sf,-}$	Downward shifted demand at time t on day s (kWh)
$d_{s,t}^{sf,+}$	Upward shifted demand at time t on day s (kWh)
$d_{s,t}^{sf}$	Shifted demand at time t on day s (kWh)
$d_{s,t}^{sd}$	Sheddable demand part of the net demand at time t on day s (kWh)
$\bar{d}_{s,t}^{sd}$	Sheddability envelope function at time t on day s (kWh)
$\bar{d}_{s,t}^{sf,+}, \bar{d}_{s,t}^{sf,-}$	Shiftability envelope functions at time t on day s (kWh)
$d_{s,t}^{sd,-}$	Sheddable demand at time t on day s (kWh)
$d_{s,t}^{flex}$	Flexible demand at time t on day s (kWh)
$\delta_{s,t}^{sf,+}, \delta_{s,t}^{sf,-}$	Auxiliary binary variables at time t on day s (kWh)
\mathbf{u}_s	Array of demand attributes $(d_t^{bl}, \bar{d}_{s,t}^{sf,+}, \bar{d}_{s,t}^{sf,-}, \bar{d}_{s,t}^{sd})$ on day s
$\boldsymbol{\theta}_s$	Array of decision variables of the s -th FOP on day s
$\boldsymbol{\theta}_t$	Array of decision variables $(d_t^{sf,+}, d_t^{sf,-}, d_t^{sd,-})$ of the consumer's problem at time t

Table 1 Notation

3.1 Components

The model considers the relationship between two parties: the consumer and the service provider. The service provider may be a retailer, aggregator, or network system operator, the distinction not being important for the general formulation. Therefore, for simplicity, we collectively refer to them as the system operator (SO). The SO is responsible for managing the consumer's transactions on the basis of net demand infor-



Figure 1 Decomposition of the observable load (by the SO) into its components: baseload demand d^{bl} , downward shifted demand $d^{sf,-}$, upward shifted demand $d^{sf,+}$ and sheddable demand d^{sd} .

mation, taken from the consumer's meter connection to the grid. We assume consumers aim to minimize their energy costs by adjusting consumption behind the meter, based on the prices they face, and they may be aided in this respect by algorithms or energy service companies. The activities behind the meter are unobserved by the SO. The specific details are outlined below:

3.1.1 Consumer

In its most general form, we assume that the consumer has baseload (inflexible) demand, some self-generation (such as rooftop solar PV panels), and some flexible demand, including storage or electric vehicle charging. The demand components are illustrated in Figure 1 and detailed below:

Net demand: The self-generation of the consumer at any time t is exogenous and random, denoted by \hat{g}_t . The electricity demand of the consumer is first served by this self-generation, if available. The rest of the demand, after taking the self-consumption and including both baseload and flexible components, is the net demand. The net demand is what the SO can observe and measure at the meter point.

Baseload demand: This component of the net demand refers to the electricity demand from the consumer which is unresponsive to price incentives. We denote this at time t , by d_t^{bl} . This has the connotation of being the necessary demand that the consumer requires at each point in time at any price below the retail market price cap, although in practice it is an empirical estimate of inflexibility across the range of prices as observed in the data.

Shiftable demand: The consumer can shift (advance or delay) some of its consumption when there are price incentives to do so. This can be done through adjusting the use of appliances such as washing machines, or interrupting the periodic requirements for heating and cooling, or making opportunistic use of battery storage and EV charging/discharging. We denote by d_t^{sf} , the shifted part of the net demand at any time t . Note that the shifted demand at any time t could be a positive or negative, respectively, denoted by $d_t^{sf,+}$ and $d_t^{sf,-}$, where $d_t^{sf} = d_t^{sf,+} - d_t^{sf,-}$, and $d_t^{sf,+} \geq 0, d_t^{sf,-} \geq 0$. The consumer receives linear price benefits $p_t^{sf,+}, p_t^{sf,-}$ per unit of energy shifted, in the positive and negative directions, respectively. However, the consumer also incurs a total cost of $c^{sf,+}(d_t^{sf,+})^2$ and $c^{sf,-}(d_t^{sf,-})^2$, respectively, for shifting in the increasing and decreasing directions at any time t . This cost would, for example, relate to the comfort or amenity loss

	Perfectly given	Stats given	Objective	Decision variables
Consumer	$\mathbf{c}, \mathbf{z}, \mathbf{u}$	$\hat{\mathbf{g}}, \hat{\mathbf{d}}$	Cost minimization	$\boldsymbol{\theta}$
SO	\mathbf{z}, \mathbf{K}_t	$\hat{\mathbf{g}}, \hat{\mathbf{d}}, \hat{\boldsymbol{\xi}}_t$	Forecast error minimization	$\boldsymbol{\theta}, \mathbf{u}$

Table 2 Describing SO's and consumer's problems

to the consumer through this shift, and the quadratic assumption is intended to reflect that it is likely to be an increasing function of scale. Finally, we assume that the load shifting in the positive and negative directions are both upper bounded by maximum values, respectively, denoted by $\bar{d}_t^{sf,+}$ and $\bar{d}_t^{sf,-}$, and referred to as ‘shiftability envelopes’.

Sheddable demand: This part of the net demand, denoted by d_t^{sd} , refers to discretionary consumption that can be entirely or partially avoided when there is a price incentive. We denote by \bar{d}^{sd} , the maximum amount of sheddable demand at any time t and by $d_t^{sd,-}$ the amount of sheddable demand that is taken. Thus, denoting by d_t^{sd} the amount of sheddable demand at time t that is still required, we have by definition $d_t^{sd} = \bar{d}^{sd} - d_t^{sd,-}$. As with shifting, the consumer receives remuneration of p_t^{sd} per unit of energy shedding but also incurs a total cost of $c^{sd}(d_t^{sd,-})^2$ for shedding demand.

3.1.2 Service provider (SO)

The consumer needs to interact with an organization for energy delivery and billing. This organization, in different jurisdictions or applications, could take a different form such as an energy retailer, an aggregator, or a network operator. We abstract away from the specific nature of this organization for the purpose of this study and we call it simply a service provide (SO). What is shared among all of these distinct forms of ‘SOs’ is that they need to have an accurate understanding and characterization of the demand components of the consumer. To be more precise, the SO can observe the net demand, but not necessarily the building blocks of the demand (i.e., sheddable, shifted, and baseload demands). Figure 1 illustrates the ‘observable’ net demand by the SO, as well as the building blocks of the net demand that may be hidden from the SO. Gaining a deeper understanding of these building blocks of the net demand, without direct measurements, would benefit the SO in many ways as indicated in the Introduction. The open question is whether and how the SO can hypothesize the building blocks of net consumption and subsequently use it for better prediction. In this work, we show how to achieve this by exploiting some exogenous information in the grid (weather information, contextual grid data, voltage, etc) in addition to the historical values of the observable net demand.

3.2 Consumer and SO problem formulations

Using the above definitions and setup, we proceed with the consumer's and SO's problem formulations. To do so, we also introduce three further notations. We define the array of ‘demand attributes’ as $\mathbf{u} :=$

$(d_t^{bl}, \bar{d}_t^{sf,+}, \bar{d}_t^{sf,-}, \bar{d}_t^{sd})_{t \in [T]}$ and the array of ‘costs’ as $\mathbf{c} = (c_t^{sf,+}, c_t^{sf,-}, c_t^{sd})_{t \in [T]}$ and the array of ‘prices’ as $\mathbf{z} = (p_t, p_t^{sf,+}, p_t^{sf,-}, p_t^{sd})_{t \in [T]}$.

3.2.1 Consumer’s cost minimization

We assume that the consumer aims to minimize its overall cost for the entire review period $[T]$. By review period, we mean the forward horizon over which it is seeking to optimize consumption. In this cost minimization, the consumer is assumed to know its cost parameters (\mathbf{c}), prices (\mathbf{z}), its flexibility potentials and baseload demand (\mathbf{u}), the historical values of its net demand ($\hat{\mathbf{d}}$), and its self-generation ($\hat{\mathbf{g}}$). With this information, the consumer decides how to activate its flexibility (i.e., shifting and shedding) to minimize the cost. We define $\boldsymbol{\theta} := (\theta_t)_{t \in [T]} = (d_t^{sf,+}, d_t^{sf,-}, d_t^{sd,-})_{t \in [T]}$ as the vector that represents the flexibility decision variables of the consumer. With this notation, we can express the consumer problem as

$$\max_{\boldsymbol{\theta} \in \Theta} \left(\ell(\boldsymbol{\theta}) := \sum_{t \in [T]} [Q_t(\theta_t) + L_t(\theta_t)] \right) \quad (1)$$

where ℓ is consumer’s utility function and Θ is the flexibility feasibility set both explained below.

The utility function ℓ defined in Eq. (1) is the cost comprising of a quadratic and a linear term, respectively, denoted by Q_t and L_t . The quadratic part represents the total comfort cost of demand shifting and shedding, $Q_t(\theta_t) := -c^{sf,+}(d_t^{sf,+})^2 - c^{sf,-}(d_t^{sf,-})^2 - c^{sd}(d_t^{sd,-})^2$. The linear part represents the financial exchanges with the SO, which is the difference between the demand flexibility gain and the consumption cost, $L_t(\theta_t) := p_t^{sf,+} d_t^{sf,+} + p_t^{sf,-} d_t^{sf,-} + p_t^{sd} d_t^{sd,-} - p_t(d_t^{bl} + d_t^{sf,+} - d_t^{sf,-} + \bar{d}_t^{sd} - d_t^{sd,-} - \hat{g}_t)$.

To understand the feasible region in which the consumer chooses its optimal flexibility decision, we define the *flexibility feasibility set*, Θ , which comprises the set of possible actions of the consumer for its flexible (shifted and sheddable) behavior. Essentially, Θ incorporates the physical upper bounds on the negative shiftability, positive shiftability, and sheddability, respectively, denoted by $\bar{d}_t^{sf,+}$, $\bar{d}_t^{sf,-}$, \bar{d}_t^{sd} , which we collectively refer to generally as *flexibility envelopes* (or resp. as *shiftability and sheddability envelopes*). These envelopes represent the physical restrictions on the maximum level of their respective flexibilities at time t . We, therefore, represent the flexibility feasibility set Θ as $\Theta(\bar{d}_t^{sf,+}, \bar{d}_t^{sf,-}, \bar{d}_t^{sd})$ to make explicit the dependence with respect to the shiftability and sheddability envelopes. Given the envelopes, the feasibility set is expressed as follows:

$$\Theta := \Theta(\bar{d}_t^{sf,+}, \bar{d}_t^{sf,-}, \bar{d}_t^{sd}) := \begin{cases} 0 \leq d_t^{sd,-} \leq \bar{d}_t^{sd} & \forall t \in [T] \\ 0 \leq d_t^{sf,+} \leq \bar{d}_t^{sf,+} \delta_t^+ & \forall t \in [T] \\ 0 \leq d_t^{sf,-} \leq \bar{d}_t^{sf,-} \delta_t^- & \forall t \in [T] \\ \sum_{t \in [T]} d_t^{sf,+} = \sum_{t \in [T]} d_t^{sf,-} & \\ \delta_t^{sf,+} + \delta_t^{sf,-} \leq 1, & \forall t \in [T] \\ \sum_{t \in [T]} (\delta_t^{sf,+} + \delta_t^{sf,-}) \leq T^{\max} & \\ \delta_t^{sf,+}, \delta_t^{sf,-} \in \{0, 1\}, & \forall t \in [T] \end{cases} \quad (2)$$

The first three lines in the feasibility set described above ensure that the shedding, positive shifting, and negative shifting, all satisfy their respective upper envelopes. In those lines, we introduce auxiliary binary variables $\delta_t^{sf,+} \in \{0, 1\}$ and $\delta_t^{sf,-} \in \{0, 1\}, t \in [T]$ to reflect practical restrictions on demand shifting. The fourth line ensures that the overall demand shifting is energy neutral and does not carry over to the next review cycle; i.e., any shifting in the positive/negative direction must be reversed before the review period is over. The fifth and sixth lines, respectively, ensure that positive and negative shifting does not occur simultaneously and that the total number of shifted hours is less than or equal to T^{\max} . Note that $T^{\max} \leq T$ represents the time flexibility of demand shifting. Large values of T^{\max} imply a larger time that the shifted demand can be spread over and hence, more time flexibility.

3.2.2 SO's forecast error minimization

The ultimate goal of the SO is to minimize the (out-of-sample) forecast error for net demand and, in the process, to estimate the consumer's unobserved demand components, including the flexibility responses/decisions, $\boldsymbol{\theta}$, and baseload demand and flexibility potentials, \mathbf{u} . We assume that the SO knows the array of price signals \mathbf{z} and physical upper bounds of the flexibility potentials, \mathbf{K} . It is generally the case that the SO has information about self generation $\hat{\mathbf{g}}$ (as these renewable facilities are usually metered separately for subsidies and/or regulatory requirements), past observed net demand measurements $\hat{\mathbf{d}}$ and various relevant weather/grid data $\hat{\boldsymbol{\xi}}$, for the entire review period $[T]$. Table 2 summarizes the problem setting.

4 Solution using inverse optimization (IO)

In this section, we first introduce the IO methodology and then explain how it can be further developed for unobservable demand response.

4.1 Theoretical background on inverse optimization

In the terminology of Inverse Optimization (IO), a *forward* optimization program (FOP) is proposed whose solutions are observed. This FOP is parametrized on some exogenous observations, \mathbf{w} , and some endogenous parameters, \mathbf{u} . Hence the formulation in a deterministic setting can be expressed as:

$$\text{FOP}(\mathbf{w}|\mathbf{u}) := \begin{cases} \max & \ell(\boldsymbol{\theta}; (\mathbf{w}|\mathbf{u})) \\ \text{s.t.} & \boldsymbol{\theta} \in \Theta(\mathbf{u}) \end{cases}, \quad (3)$$

where for any value of \mathbf{u} , we assume that $\Theta(\mathbf{u})$ is a closed convex set and ℓ a differentiable and concave utility function with respect to $\boldsymbol{\theta}$.

In a non-deterministic setting (such as our problem), the IO solution must consider the observation noise, such that the IO model becomes a supervised learning problem with multivariate output. More formally, therefore, the training dataset, \mathcal{D} , is built up by S pairs of observations $\mathcal{D}_S := \{(\mathbf{w}_s, \boldsymbol{\theta}_s)\}_{s \in [S]}$ and the goal is to find $\hat{\mathbf{u}}$ that would make $\boldsymbol{\theta}_s$ "optimal" for the s -th FOP. That is, $\text{FOP}(\mathbf{z}_s|\hat{\mathbf{u}})$. Thus, having estimated the parameter \mathbf{u} by $\hat{\mathbf{u}}$, and given a new observation \mathbf{w}' , $\text{FOP}(\mathbf{w}'|\hat{\mathbf{u}})$ is used to estimate $\boldsymbol{\theta}'$ (Saez-Gallego and Morales 2017).

4.2 Applying IO to unobservable demand response

The FOP model is naturally delivered by the consumer's problem as defined in Eq. (1). Adapting the basic approach as described above, we proceed in detail, as follows:

4.2.1 The forward or reconstruction program

Given the training dataset $\mathcal{D}_S := \{((\mathbf{c}_s, \mathbf{z}_s, \hat{\mathbf{g}}_s), \hat{\mathbf{d}}_s)\}_{s \in [S]}$ made by S training samples (which may correspond to a set of days), built on pairs of T -dimensional exogenous observations (cost, price and self generation data), $(\mathbf{c}_s, \mathbf{z}_s, \hat{\mathbf{g}}_s)$, and observed load measurements $\hat{\mathbf{d}}_s$. In this setting, $(\mathbf{c}_s, \mathbf{z}_s, \hat{\mathbf{g}}_s)$ plays the role of \mathbf{w} in program (3). Thus, the data-driven IO model tries to find estimates of demand attributes $\hat{\mathbf{u}}_s$ of the parameters $\mathbf{u}_s = (d_t^{bl}, \bar{d}_{s,t}^{sf,+}, \bar{d}_{s,t}^{sf,-}, \bar{d}_{s,t}^{sd})$ which would make the observed s -th demand $\hat{\mathbf{d}}_s$ "optimal" for the s -th FOP defined as follows:

$$\text{FOP}((\mathbf{c}_s, \mathbf{z}_s, \hat{\mathbf{g}}_s) | \mathbf{u}_s) := \begin{cases} \max & \ell(\boldsymbol{\theta}_s; ((\mathbf{c}_s, \mathbf{z}_s, \hat{\mathbf{g}}_s) | \mathbf{u}_s)) \\ \text{s.t.} & \boldsymbol{\theta}_s = (\mathbf{d}_s^{sf,+}, \mathbf{d}_s^{sf,-}, \mathbf{d}_s^{sd,-}) \in \Theta(\bar{d}_{s,t}^{sf,+}, \bar{d}_{s,t}^{sf,-}, \bar{d}_{s,t}^{sd}) \\ & d_{s,t}^{sf} = d_{s,t}^{sf,+} - d_{s,t}^{sf,-} \quad \forall t \in [T] \\ & d_{s,t}^{sd} = \bar{d}_{s,t}^{sd} - d_{s,t}^{sd,-} \quad \forall t \in [T] \end{cases} \quad (4)$$

Having introduced the end-users' FOP, next we explain how the proposed framework works: (i) a *learning step* where the data-driven IO model is fitted by using a training dataset, and (ii) a *forecasting step* where the time-series forecast output is computed.

4.2.2 Learning

Having observed a time series given by set of $[S]$ days of the demand per time period t , $\{(\hat{d}_{s,t})_{t \in [T]}\}_{s \in [S]}$, which form the training dataset, the learning step is given by the solution of the following data-driven inverse optimization program:

$$\min \sum_{s \in [S]} \omega_s \left\| \left([\mathbf{d}^{bl} + \mathbf{d}_s^{sf} + \mathbf{d}_s^{sd} - \hat{\mathbf{g}}_s] - \hat{\mathbf{d}}_s \right)_s \right\|_p^p \quad (5a)$$

$$\text{s.t. } d_{s,t}^{sf} = d_{s,t}^{sf,+} - d_{s,t}^{sf,-} \quad \forall s \in [S], \forall t \in [T] \quad (5b)$$

$$d_{s,t}^{sd} = \bar{d}_{s,t}^{sd} - d_{s,t}^{sd,-} \quad \forall s \in [S], \forall t \in [T] \quad (5c)$$

$$0 \leq d_t^{bl} \quad \forall t \in [T] \quad (5d)$$

$$0 \leq \bar{d}_{s,t}^{sf,+} \leq K_{s,t}^{sf,+} \quad \forall s \in [S], \forall t \in [T] \quad (5e)$$

$$0 \leq \bar{d}_{s,t}^{sf,-} \leq K_{s,t}^{sf,-} \quad \forall s \in [S], \forall t \in [T] \quad (5f)$$

$$0 \leq \bar{d}_{s,t}^{sd} \leq K_{s,t}^{sd} \quad \forall s \in [S], \forall t \in [T] \quad (5g)$$

$$\delta_{s,t}^{sf,+}, \delta_{s,t}^{sf,-} \in \{0, 1\} \quad \forall s \in [S], \forall t \in [T] \quad (5h)$$

$$\delta_{s,t}^{sf,+} + \delta_{s,t}^{sf,-} \leq 1 \quad \forall s \in [S], \forall t \in [T] \quad (5i)$$

$$\sum_{t \in [T]} (\delta_{s,t}^{sf,+} + \delta_{s,t}^{sf,-}) \leq T^{\max} \quad \forall s \in [S] \quad (5j)$$

$$\boldsymbol{\theta}_s := (\mathbf{d}^{sf,+}, \mathbf{d}^{sf,-}, \mathbf{d}^{sd,-})_s \quad \forall s \in [S] \quad (5k)$$

$$\mathbf{u}_s = (d_t^{bl}, \bar{d}_{s,t}^{sf,+}, \bar{d}_{s,t}^{sf,-}, \bar{d}_{s,t}^{sd}) \quad (5l)$$

$$\boldsymbol{\theta}_s \in \arg \max \ell(\boldsymbol{\theta}_s; ((\mathbf{c}_s, \mathbf{z}_s, \hat{\mathbf{g}}_s) | \mathbf{u}_s)) \quad (5m)$$

$$\text{s.t. } \sum_{t \in [T]} d_{s,t}^{sf,+} = \sum_{t \in [T]} d_{s,t}^{sf,-} \quad : \quad (\kappa_s) \quad (5n)$$

$$d_{s,t}^{sf,+} \leq \bar{d}_{s,t}^{sf,+} \delta_{s,t}^{sf,+} \quad : \quad (\mu_{s,t}^+ \geq 0) \quad \forall t \in [T] \quad (5o)$$

$$d_{s,t}^{sf,-} \leq \bar{d}_{s,t}^{sf,-} \delta_{s,t}^{sf,-} \quad : \quad (\mu_{s,t}^- \geq 0) \quad \forall t \in [T] \quad (5p)$$

$$d_{s,t}^{sd,-} \leq \bar{d}_{s,t}^{sd} \quad : \quad (\mu_{s,t}^0 \geq 0) \quad \forall t \in [T] \quad (5q)$$

$$0 \leq d_{s,t}^{sf,+} \quad : \quad (\mathbf{v}_{s,t}^+ \geq 0) \quad \forall t \in [T] \quad (5r)$$

$$0 \leq d_{s,t}^{sf,-} \quad : \quad (\mathbf{v}_{s,t}^- \geq 0) \quad \forall t \in [T] \quad (5s)$$

$$0 \leq d_{s,t}^{sd,-} \quad : \quad (\mathbf{v}_{s,t}^0 \geq 0) \quad \forall t \in [T] \quad (5t)$$

where $\|\cdot\|_p$, with $p > 1$, denotes the p -norm, ω_s is the weight of the forecast error on day $s \in [S]$ (Saez-Gallego et al. 2016) and the variables in parenthesis in the constraints of the s -th lower level problem denote the respective dual variables. We set $\omega_s := \left(\frac{s}{S}\right)^\alpha / \left(\sum_{s' \in [S]} \left(\frac{s'}{S}\right)^\alpha\right)$ the normalized weights of the training days, with $\alpha \geq 0$ the forgetting factor parameter to represent discounting older data. If $\alpha = 0$, then all observations are equally weighted and when α increases, more weight is given to recent observations, as suggested by Saez-Gallego et al. (2016), Lu et al. (2018).

The flexibility envelopes $\bar{d}_{s,t}^{sf,+}$, $\bar{d}_{s,t}^{sf,-}$ and $\bar{d}_{s,t}^{sd}$, which are upper bounded by the input parameters $K_{s,t}^{sf,+}$, $K_{s,t}^{sf,-}$ and $K_{s,t}^{sd}$, respectively (in the numerical experiments are equal to the absolute value of the observed demand, $|\hat{d}_{s,t}|$), are random functions themselves because they may evolve over time from day to day, and hence, should be estimated from past data. To do so, we follow the approach introduced by Fernández-Blanco et al. (2021b), which proposes a decision rule based on a Gaussian Kernel function to capture the non-linear dependence between regressors and power:

$$\bar{d}_{s,t}^{sf,+} = \beta_0^{sf,+} + \sum_{s' \in [S]} \sum_{t' \in [T]} \beta_{s',t'}^{sf,+} \exp\left(-\gamma^{sf,+} \left\| \hat{\boldsymbol{\xi}}_{s,t} - \hat{\boldsymbol{\xi}}_{s',t'} \right\|\right) \quad (6)$$

$$\bar{d}_{s,t}^{sf,-} = \beta_0^{sf,-} + \sum_{s' \in [S]} \sum_{t' \in [T]} \beta_{s',t'}^{sf,-} \exp\left(-\gamma^{sf,-} \left\| \hat{\boldsymbol{\xi}}_{s,t} - \hat{\boldsymbol{\xi}}_{s',t'} \right\|\right) \quad (7)$$

$$\bar{d}_{s,t}^{sd} = \beta_0^{sd} + \sum_{s' \in [S]} \sum_{t' \in [T]} \beta_{s',t'}^{sd} \exp\left(-\gamma^{sd} \left\| \hat{\boldsymbol{\xi}}_{s,t} - \hat{\boldsymbol{\xi}}_{s',t'} \right\|\right) \quad (8)$$

where $\gamma^{sf,+}, \gamma^{sf,-}, \gamma^{sd} > 0$ are the Gaussian kernel bandwidth parameter associated to $\bar{d}_{s,t}^{sf,+}$, $\bar{d}_{s,t}^{sf,-}$ and $\bar{d}_{s,t}^{sd}$ respectively. Moreover, $\hat{\boldsymbol{\xi}}_s$ is the vector of external features (for example weather information or contextual grid data, etc) corresponding to day s at hour t of the inverse optimization program used to estimate the maximum availability of flexible demand at time t on day s .

4.3 Component estimation and forecasting

Having introduced the parameterizations in terms of the kernels and the decision variables for the flexibility envelopes, we compute $\hat{\mathbf{d}}^{bl}$ and $\hat{\boldsymbol{\beta}}$ being the optimal solutions of \mathbf{d}^{bl} and $\boldsymbol{\beta} := [\boldsymbol{\beta}_0^{sf,+}, \boldsymbol{\beta}_0^{sf,-}, \boldsymbol{\beta}_0^{sd}, (\boldsymbol{\beta}_s^{sf,+}, \boldsymbol{\beta}_s^{sf,-}, \boldsymbol{\beta}_s^{sd})_{s \in [S]}]$ in the problem defined by (5a)-(5t), respectively. Thus, we can compute $\hat{\mathbf{u}} := (\hat{\mathbf{d}}^{bl}, \bar{d}_{S+1,t}^{sf,+}, \bar{d}_{S+1,t}^{sf,-}, \bar{d}_{S+1,t}^{sd})$ where

$$\bar{d}_{S+1,t}^{sf,+} = \max \left(\hat{\beta}_0^{sf,+} + \sum_{s' \in [S]} \sum_{t' \in [T]} \hat{\beta}_{s',t'}^{sf,+} \exp \left(-\gamma^{sf,+} \left\| \hat{\boldsymbol{\xi}}_{S+1,t} - \hat{\boldsymbol{\xi}}_{s',t'} \right\| \right), 0 \right) \quad (9)$$

$$\bar{d}_{S+1,t}^{sf,-} = \max \left(\hat{\beta}_0^{sf,-} + \sum_{s' \in [S]} \sum_{t' \in [T]} \hat{\beta}_{s',t'}^{sf,-} \exp \left(-\gamma^{sf,-} \left\| \hat{\boldsymbol{\xi}}_{S+1,t} - \hat{\boldsymbol{\xi}}_{s',t'} \right\| \right), 0 \right) \quad (10)$$

$$\bar{d}_{S+1,t}^{sd} = \max \left(\hat{\beta}_0^{sd} + \sum_{s' \in [S]} \sum_{t' \in [T]} \hat{\beta}_{s',t'}^{sh} \exp \left(-\gamma^{sd} \left\| \hat{\boldsymbol{\xi}}_{S+1,t} - \hat{\boldsymbol{\xi}}_{s',t'} \right\| \right), 0 \right) \quad (11)$$

Having computed $\hat{\mathbf{u}}$, the forecast output for the day $S+1$ is given by solving the following forward program given the exogenous observations for the day $S+1$, that is cost, price and local generation data on day $S+1$, $(\mathbf{c}_{S+1}, \mathbf{z}_{S+1}, \hat{\mathbf{g}}_{S+1})$:

$$\begin{aligned} & \max \ell(\boldsymbol{\theta}_{S+1}; ((\mathbf{c}_{S+1}, \mathbf{z}_{S+1}, \hat{\mathbf{g}}_{S+1}) | \hat{\mathbf{u}})) \\ & \text{s.t. } d_{S+1,t}^{sf,+} = \bar{d}_{S+1,t}^{sf,+} - d_{S+1,t}^{sf,-} & \forall t \in [T] \\ & \quad d_{S+1,k,t}^{sd} = \bar{d}_{S+1,t}^{sd} - d_{S+1,t}^{sd,-} & \forall t \in [T] \\ & \quad \boldsymbol{\theta}_{S+1} = (\mathbf{d}^{sf,+}, \mathbf{d}^{sf,-}, \mathbf{d}^{sd,-})_{S+1} \in \Theta(\bar{d}_{S+1,t}^{sf,+}, \bar{d}_{S+1,t}^{sf,-}, \bar{d}_{S+1,t}^{sd}) \end{aligned}$$

After solving the above program and getting $(\mathbf{d}^{sf,+}, \mathbf{d}^{sf,-}, \mathbf{d}^{sd,-})_{S+1}$, we can compute the forecast net load per time t for day $S+1$, $\hat{d}_{S+1,t}$, as the sum of the (net) baseload demand, $\hat{d}_t^{bl} - \hat{g}_{S+1,t}$, plus the flexible demand, $d_{S+1,t}^{flex} := d_{S+1,t}^{sf,+} + d_{S+1,t}^{sd}$ as follows:

$$\hat{d}_{S+1,t} := (\hat{d}_t^{bl} - \hat{g}_{S+1,t}) + d_{S+1,t}^{flex} \quad (12)$$

The next section develops a single-level tractable reformulation by exploiting the Karush-Kuhn-Tucker (KKT) conditions for the lower-level and the underlying conic structure of the data-driven IO problem.

4.4 Single-level conic reformulation

The Karush-Kuhn-Tucker (KKT) conditions for the lower-level problem enables us to reformulate the IO model as a single-level optimization program:

$$\min \sum_{s \in [S]} \omega_s u_s \quad (13a)$$

$$\text{s.t. } u_s \geq \left\| \left(\mathbf{d}^{bl} + \mathbf{d}_s^{sf} + \mathbf{d}_s^{sd} - \hat{\mathbf{g}}_s - \hat{\mathbf{d}}_s \right) \right\|_s \Big|_p \quad \forall s \in [S] \quad (13b)$$

$$(5b) - (5g) \quad (13c)$$

$$(6), (7), (8) \quad \forall s \in [S], \forall t \in [T] \quad (13d)$$

$$-2c_{s,t}^{sf,+} d_{s,t}^{sf,+} + p_{s,t}^{sf,+} - p_{s,t} + \kappa_s - \mu_{s,t}^+ + v_{s,t}^+ = 0 \quad \forall s \in [S], \forall t \in [T] \quad (13e)$$

$$-2c_{s,t}^{sf,-} d_{s,t}^{sf,-} + p_{s,t}^{sf,-} + p_{s,t} - \kappa_s - \mu_{s,t}^- + v_{s,t}^- = 0 \quad \forall s \in [S], \forall t \in [T] \quad (13f)$$

$$-2c_{s,t}^{sd} d_{s,t}^{sd,-} + p_{s,t}^{sd} + p_{s,t} - \mu_{s,t}^0 + v_{s,t}^0 = 0 \quad \forall s \in [S], \forall t \in [T] \quad (13g)$$

$$\mu_{s,t}^+ (\bar{d}_{s,t}^{sf,+} \delta_{s,t}^{sf,+} - d_{s,t}^{sf,+}) = 0 \quad \forall s \in [S], \forall t \in [T] \quad (13h)$$

$$\mu_{s,t}^- (\bar{d}_{s,t}^{sf,-} \delta_{s,t}^{sf,-} - d_{s,t}^{sf,-}) = 0 \quad \forall s \in [S], \forall t \in [T] \quad (13i)$$

$$\mu_{s,t}^0 (\bar{d}_{s,t}^{sd} - d_{s,t}^{sd,-}) = 0 \quad \forall s \in [S], \forall t \in [T] \quad (13j)$$

$$v_{s,t}^0 d_{s,t}^{sd,-} = 0 \quad \forall s \in [S], \forall t \in [T] \quad (13k)$$

$$v_{s,t}^+ d_{s,t}^{sf,+} = 0 \quad \forall s \in [S], \forall t \in [T] \quad (13l)$$

$$v_{s,t}^- d_{s,t}^{sf,-} = 0 \quad \forall s \in [S], \forall t \in [T] \quad (13m)$$

$$\mu_{s,t}^+, \mu_{s,t}^-, \mu_{s,t}^0, v_{s,t}^+, v_{s,t}^-, v_{s,t}^0 \geq 0 \quad \forall s \in [S], \forall t \in [T] \quad (13n)$$

$$\theta_s \in \Theta(\bar{d}_{s,t}^{sf,+}, \bar{d}_{s,t}^{sf,-}, \bar{d}_{s,t}^{sd}) \quad \forall s \in [S] \quad (13o)$$

$$\kappa_s \in \mathbb{R}, u_s \geq 0 \quad \forall s \in [S] \quad (13p)$$

The above program can be recast as a mixed-integer conic-constrained program solvable by off-the-shelf conic optimization software such as MOSEK (MOSEK 2024). The complementary conditions can be rewritten as special ordered sets of type 1 constraints (SOS1), which are a set of non-negative variables that only one of them can be positive, by avoiding the need to select the big-M parameters for the complementary conditions without jeopardizing the computational performance (Kleinert and Schmidt 2023, Siddiqui and Gabriel 2013). Also, the above objective function via the p -norms can be reformulated as S conic constraints amenable for the efficient conic solver of MOSEK. For the applications below, we consider $p = 2$, and hence the above problem defined by (13a)-(13p) can be modeled as a mixed-integer program with linear objective function and S rotated conic quadratic constraints amenable for MOSEK.

5 Empirical research

Using the above IO methodology, the logical flow of the empirical research questions that we address are as follows:

Q1: Using net demand with structural assumptions and a presumed optimization model for the flexible and baseload components of domestic demand and their price responses, how well is the above IO formulation able to estimate the latent components of flexible and baseload demand? This will establish proof of concept and computational tractability.

Q2: Can the resulting latent component estimates from IO be accurately predicted out of sample, using market-wide information such as weather and periodic effects, but without assuming knowledge of the appliance activities? The predictability of the components needs to be established against benchmark statistical and machine learning methods.

Q3: Are forecasts of net demand obtained by summing the latent components more accurate than forecasts of the aggregate net demand series? This is needed to validate the value of the decomposed approach for forecasting.

Q4: With data that provides explicit knowledge of the domestic appliance activities, do these latent components from IO have a credible relationship to the appliance activities and thereby appear valid? Plausible statistical relationships to the data will establish construct validity.

Q5: Overall, can the price response of domestic customers be more accurately estimated based upon an IO decomposition of flexible and baseload components than by conventional benchmark methods? This is needed to justify the overall proposition that IO can be useful in practice compared to benchmark forecasting methods.

We progress the analysis of Q1-Q5 through two data sets for clarity of focus. For the first part, Q1 to Q4, we use a set of smart household data, compiled by [Singh \(2024\)](#) and openly available on the Kaggle platform to facilitate replication studies. It contains the smart meter readings in kW from a US household of all of the main household appliances at minute-by-minute granularity for 350 days of house appliances, together with the weather conditions of that particular region. It does not contain any retail price data. We do however know the typical retail prices for that region (Ohio) in 2018. This example replicates the perspective of a network operator who would not know the retailer-customer tariff details precisely. We use this to test the application of the IO approach and sense-check the identified components of flexible and inflexible components against actual appliance use. The forecasting questions are also evaluated on this data, but for Q5, which relies upon precise TOU responses, we use consumer data from Japan, made available by [Kiguchi et al. \(2021\)](#). This is intraday net load data from a sample of customers responding to price signals for several months in 2018. This example therefore replicates the other case of a retailer setting TOU tariffs, observing the metered net loads but not knowing exactly how the appliances were being used. The logic of our analysis is, therefore, that having established the construct validity of the component estimates on the first data set, we are justified in applying it in the second data set in order to compare its forecasting performance under TOU prices against conventional benchmarks.

The IO method is benchmarked against two classical time-series models SARIMA, SARIMAX, and also against a non-linear method, XGboost ([Chen and Guestrin 2016](#)). For the SARIMAX and SARIMA, we choose the parameters that minimize the AIC (the choice (2, 1, 2, 6) seems reasonably well in all cases). XGboost is applied by using the skforecast Python package ([Amat Rodrigo and Escobar Ortiz 2024](#)) via default options with 6 lags.

The performance metrics used for evaluations of the forecasts are the usual mean absolute error (MAE) and the root mean square error (RMSE) defined as follows:

$$\text{MAE}(d^{true}, d^{fo}) = \frac{1}{|T^{fo}|} \sum_{t \in T^{fo}} |d_t^{true} - d_t^{fo}| \quad (14)$$

$$\text{RMSE}(d^{true}, d^{fo}) = \sqrt{\frac{1}{|T^{fo}|} \sum_{t \in T^{fo}} (d_t^{true} - d_t^{fo})^2} \quad (15)$$

where d^{true}, d^{fo} are the load measurements and forecast values, and T^{fo} is the planning horizon set (in our case, 5 days of 24 hours). We assume that on every day at hour t the external regressors are perfectly known. This is often assumed in forecasting research in order to focus more directly upon the comparative methodologies so that the results are not confounded by estimation errors in variables. Computations were performed on a Windows-based laptop with 4 cores and 8 logical processors clocking at 2.6 GHz and 16 GB of RAM using the solver MOSEK under Pyomo (Bynum et al. 2021). The IO model depends on five hyperparameters, namely: $param = [T^{\max}, \alpha, \gamma^{f,+}, \gamma^{f,-}, \gamma^d]$, which were tuned via a grid-search.

5.1 Performance effectiveness and construct validity

The smart household data from Singh (2024) is used to test the empirical performance of the proposed IO method against conventional benchmarks. It also allows us to check that the identified flexible and baseload components do in fact represent what they are intended to model, i.e., that they have construct validity. We do that by regressing the estimated flexible and baseload component activities on the known usage of household appliances as well as autoregressive lags. We expect the discretionary use of appliances to feature more strongly in the flexible component but less so in the baseload component, whilst the autoregressive effects would relate to adaptation and habit and should feature more strongly in the baseload component. The data measurements include the kitchen appliances (e.g. fridge, dishwasher, microwave), various rooms (e.g. kitchen, living room, home office), furnace, well, barn, garage door, etc., as well as solar generation and weather conditions. The minute-by-minute data is from a sample of US households in Ohio taken over 2018 (as also analyzed in Tlenshiyeva et al. (2024)). We restrict the analysis to weekdays. Seasonality is captured with sine and cosine functions and the temperature regressor is defined by $Tdiff := \frac{T - T^{app}}{\log T - \log T^{app}}$ and then scaled between -0.5 and 0.5. Recap that the net load is consumed energy minus the solar generation.

Even though we do not know the precise tariff details for the customer, we expect the IO method to be robust to noisy assumptions and we introduce a typical tariff for that location at that time (based upon inspection of published rates from various local utilities). We estimated a typical flat tariff of 22 c/kWh and prices of 29 c/kWh and 15 c/kWh for the peak and off-peak periods, with the peak defined as 2 – 6 pm in summer and 6 – 9 am in winter. We also define $p_t^{sf,+} = \max(p_t - \text{TOU}_t, 0)$, $p_t^{sf,-} = \max(\text{TOU}_t - p_t, 0)$. The parameters for load shedding are defined by $\sum_{t \in [T]} p_t^{sf,+} / 24$. The parameters $c_t^{sf,+}, c_t^{sf,-}$ are set to $|p_t - \text{TOU}_t|$ when $p_t^{sf,+}, p_t^{sf,-}$ are equal to zero, respectively, and 0, otherwise. The training data uses two months, weekdays only, and the goal is to predict the first five days of the next month. We consider four seasonal sets of results.

Figure 2 shows the net demand (demand is referred to as load in the Kaggle data source) for the four cases (upper left January to March, upper right April to June, lower left July to September, and lower right

October to December) under the optimal hyperparameter tuning via grid-search. Similarly, Figures 3 and 4 show the net baseload demand and flexible profiles estimated as part of the modeling. We also include the summary results in Tables 3-4.

In all figures, the peak price periods are shown shaded in pink. Whilst the effect of peak pricing is not evident in the net load profiles shown in Figure 2, nor in the baseload components shown in Figure 3, it is very evident in Figure 4. In Figure 4, we can see that only the IO approach is showing a distinct reduction in the flexible load component during the hours of peak pricing. This is, of course, what we would hope to see, as the IO approach is designed to identify this component. Visually, it is a very reassuring display that the IO is indeed providing a new component that the benchmark methods cannot reveal. It is also interesting to see in Figure 4 that during the Summer, the flexible load reduction is compensated by prior increases in load, whereas in the winter it is compensated with load increases afterwards. This seasonal distinction in the pattern of demand shifting is a new insight revealed by the methodology.

Regarding relative accuracy, according to Tables 3, for Winter, IO demonstrates the lowest MAE (0.2170) and RMSE (0.2877) for the “Net load” category, outperforming all the benchmark methods. SARIMA and SARIMAX have higher MAE and RMSE values in comparison to IO but still outperform XGBoost in the same category. XGBoost shows the highest errors across most categories. Tables 4 shows that the results for summer exhibit slight shift. While IO maintained the lowest MAE (0.1689) and RMSE (0.2362) for “Net load”, SARIMA and SARIMAX performed comparably but with higher errors than IO. XGBoost again shows the highest MAE and RMSE for “Net load” but does well for the d^{bl} with the lowest errors among the SARIMA and SARIMAX methods.

According to these figures, IO demonstrates the most accurate performance across all seasons, consistently achieving the lowest errors in the “Net load”. SARIMA and SARIMAX generally follow, with SARIMA showing a slight edge over SARIMAX in some cases. Surprisingly, XGBoost, despite having some strong performances in d^{bl} and d^{flex} , often has the highest errors for “Net load” metrics. Most importantly for our purposes, from Figures 3 and 4 it is evident that the baseload component is more regular and predictable than the flexible component, which is intuitive and reassuring. Overall, these results appear to convincingly support research questions, Q1 and Q2, in establishing the feasibility and comparative value of the IO approach.

In relation to Q3, which focuses upon the inherent modeling element of predicting the components separately, and then summing to get the Net load forecast, Tables 3-4 also report some justification. The rows designated Net Load and Net Load 2 display the accuracies for predicting on the basis only of the aggregate Net Load data versus the disaggregated approach of predicting the components and summing. Across the two seasons, the methods show varying degrees of improvement from “Net load” to “Net load 2”. XGBoost demonstrated substantial improvements, with reductions in MAE ranging from approximately 38.9% in Winter to 26.6% in Summer, and reductions in RMSE from approximately 37.3% in Winter to 28.0% in

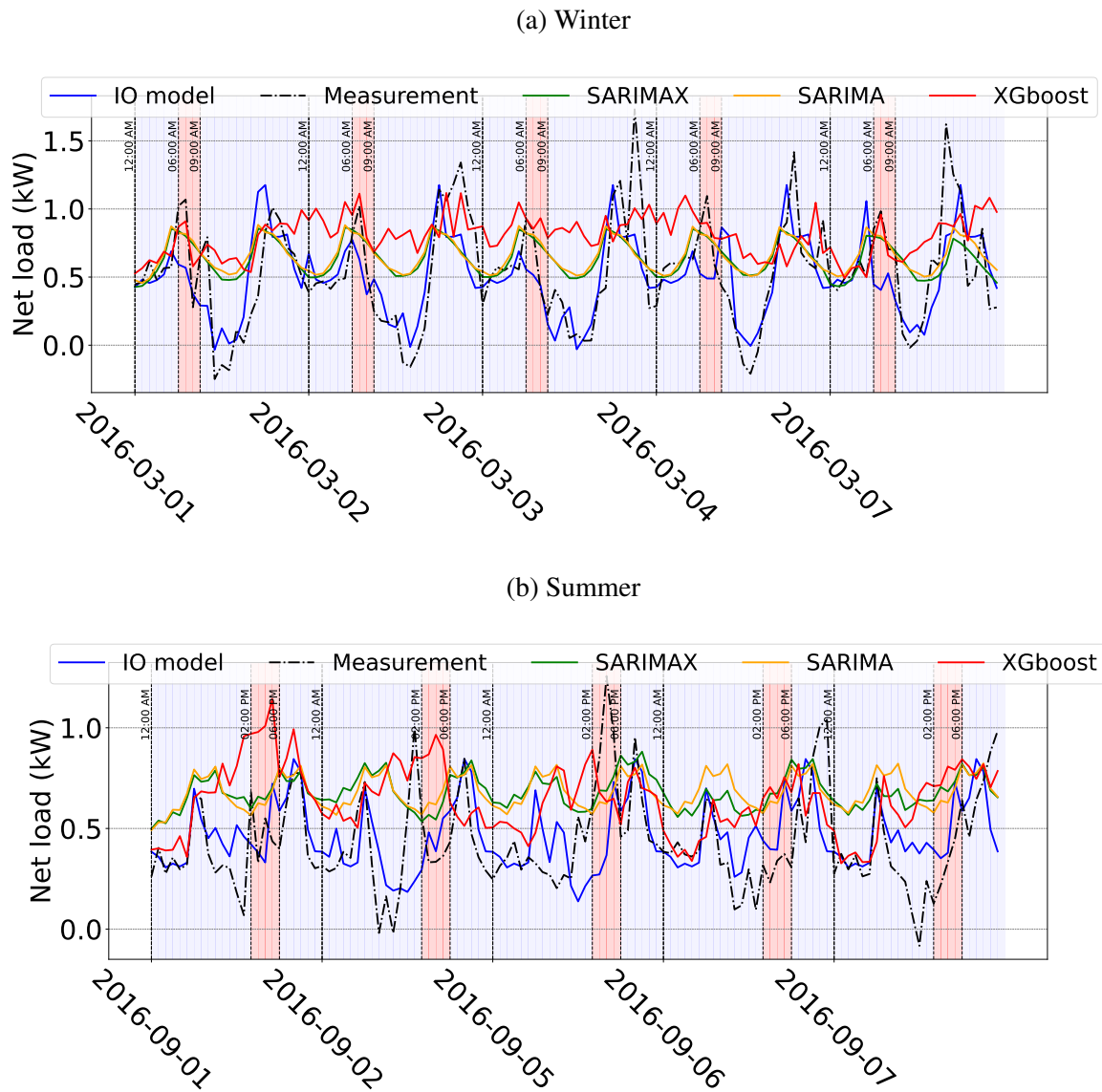


Figure 2 Net load profiles and performance error metrics under best hyperparameter tuning

Summer. SARIMA also shows notable improvements, with MAE reductions of about 20.5% in Winter and 46.5% in Summer, and RMSE reductions of about 18.8% in Winter and 36.7% in Summer. SARIMAX exhibited consistent improvements, with MAE reductions from 26.9% in Winter to 37.4% in Summer, and RMSE reductions from 27.8% in Winter to 28.0% in Summer. Overall, all methods generally performed better with “Net load 2,” with XGBoost and SARIMA showing the most significant improvements. In other words, the principle of component-based forecasting appears to be justified.

Finally, whilst the error metrics for the point forecasts validate the relative accuracy of the IO approach for forecasting, it is becoming increasingly important in demand forecasting to understand the tail risks in predictions. This involves producing density forecasts and assessing the calibrations of the predicted quantiles. For this purpose, we report the conventional continuous rank probability scores (CRPS) averaged

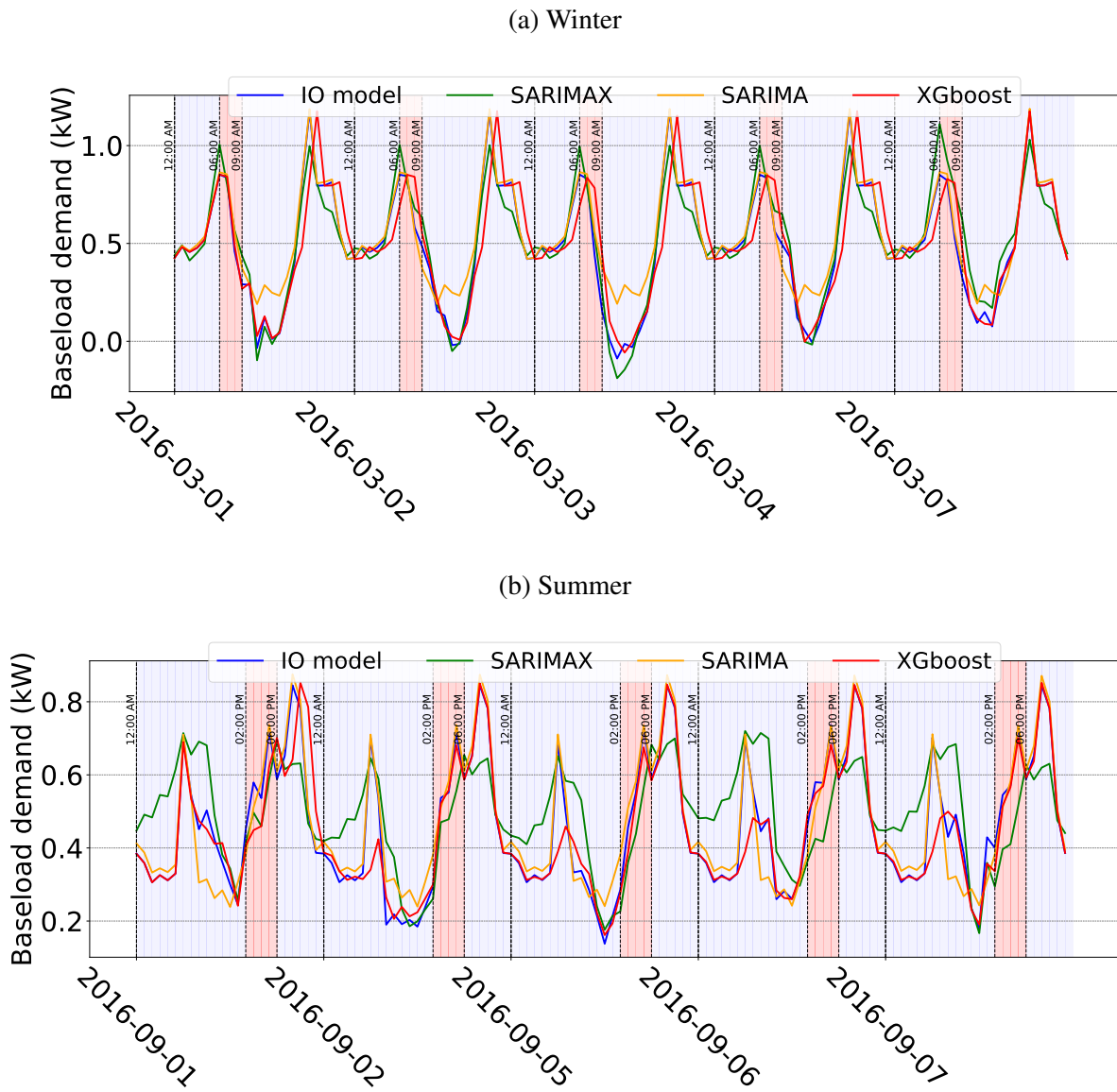


Figure 3 Net baseload demand profiles and performance error metrics under best hyperparameter tuning

Table 3 Error metrics for Winter

	IO		XGboost		SARIMA		SARIMAX	
	MAE	RMSE	MAE	RMSE	MAE	RMSE	MAE	RMSE
Net load	0.2170	0.2877	0.3734	0.4611	0.2835	0.3619	0.2995	0.3881
d^{bl}	-	-	0.0906	0.1476	0.0590	0.0994	0.0703	0.0910
d^{flex}	-	-	0.1895	0.2197	0.0998	0.1383	0.1051	0.1531
Net load 2	0.2170	0.2877	0.2281	0.2890	0.2255	0.2936	0.2189	0.2801

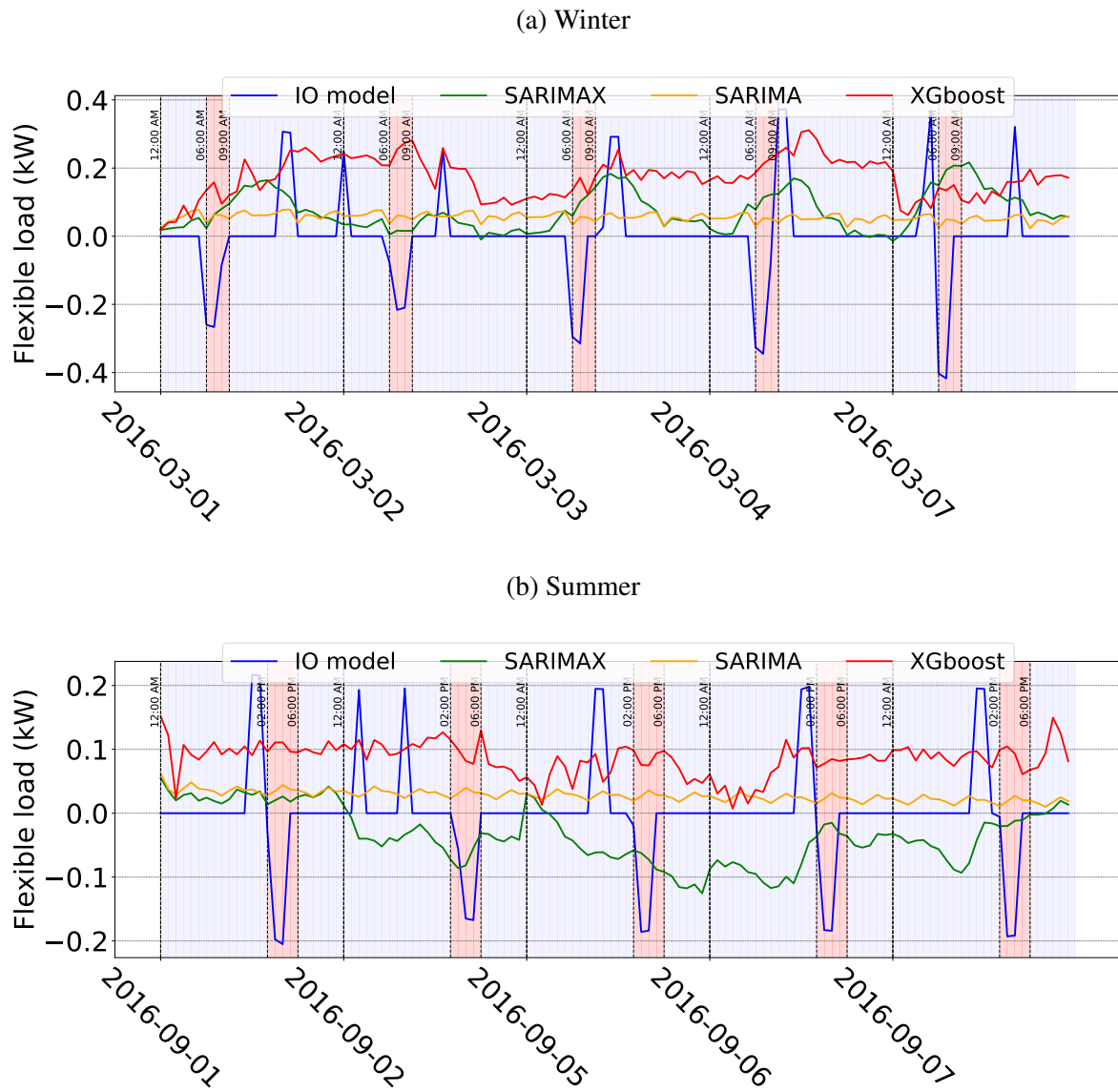


Figure 4 Flexible load profiles and performance error metrics under best hyperparameter tuning

Table 4 Error metrics for Summer

	IO		XGboost		SARIMA		SARIMAX	
	MAE	RMSE	MAE	RMSE	MAE	RMSE	MAE	RMSE
Net load	0.1689	0.2362	0.2824	0.3458	0.3070	0.3464	0.2990	0.3399
d^{bl}	-	-	0.0363	0.0762	0.0401	0.0508	0.1104	0.1332
d^{flex}	-	-	0.1028	0.1186	0.0564	0.0848	0.07120	0.0971
Net load 2	0.1689	0.2362	0.2073	0.2488	0.1642	0.2192	0.1871	0.2446

Table 5 Error metrics for the net load probabilistic forecasting: Quantiles and CRPS

	IO			XGboost			SARIMA			SARIMAX		
	$q_{0.05}$	$q_{0.95}$	CRPS	$q_{0.05}$	$q_{0.95}$	CRPS	$q_{0.05}$	$q_{0.95}$	CRPS	$q_{0.05}$	$q_{0.95}$	CRPS
Winter	0.337	1.044	0.219	0.658	1.109	0.362	0.523	1.114	0.297	0.515	1.121	0.293
Summer	0.271	0.815	0.131	0.393	1.046	0.238	0.379	1.014	0.181	0.379	1.008	0.181

over the forecast horizon T^{fo} . CRPS is a strictly proper scoring rule which is widely used within density forecasting research. It needs to be approximated in practice, and one approach is based on exploiting its equivalent quantile-based representation [Gneiting and Ranjan \(2011\)](#):

$$\text{CRPS}(F, y) = 2 \int_0^1 \text{QL}_q(F^{-1}(q), y) dq \quad (16)$$

where F, F^{-1} are the distribution and quantile function, respectively, y is the measurement, and QL is the quantile loss function. Computing the proxy for CRPS requires the q -quantiles, where $q \in \{0.01, 0.05, \dots, 0.95, 0.99\}$. We used the forecasting method with the pinball loss function (also known as quantile score function) available in [\(Amat Rodrigo and Escobar Ortiz 2024\)](#).

Table 5 contains the 0.05, 0.95-quantiles, $q_{0.05}, q_{0.95}$, and the CRPS (averaged over the forecast horizon). Note that lower scores are better and we observe that the IO method outperforms very substantially across all seasons. SARIMA and SARIMAX generally have intermediate performance, with minor differences between them. Overall, the superior fitting and forecasting accuracy of the IO method for Net load appears to be well established against conventional benchmarks, in terms of both average accuracy and predictive density calibration. This established the feasibility and overall merit of the approach. The next question (Q4) is whether the estimated components really do represent what they are intended to represent, i.e., their construct validity.

To assess the construct validity of the flexible and baseload components delivered by the IO method, we regress each estimated component time series on the known metered appliance activities to assess their relative impact on the component's variation. We use the conventional Shapley values to represent the relative feature importance of the appliance activities. In this way, we can see if the IO method provides meaningful load decompositions. Figures 5 and 6 display the relative feature strength of each appliance on the baseload and flexible components. The features are ranked by their importance. Figure 5 reveals that the baseload component does not depend so much upon the discretionary use of appliances, but on the adaptive habitual consumption, as indicated by the autoregressive lags and the regular solar generation. For the flexible load component, the reverse pattern is revealed. Figure 6 shows the importance of the appliances, particularly the flexible ones, such as the dishwasher, whilst the autoregressive terms are not featured. Hence, we claim that the IO results provide a meaningful load decomposition into the flexible and baseload components.

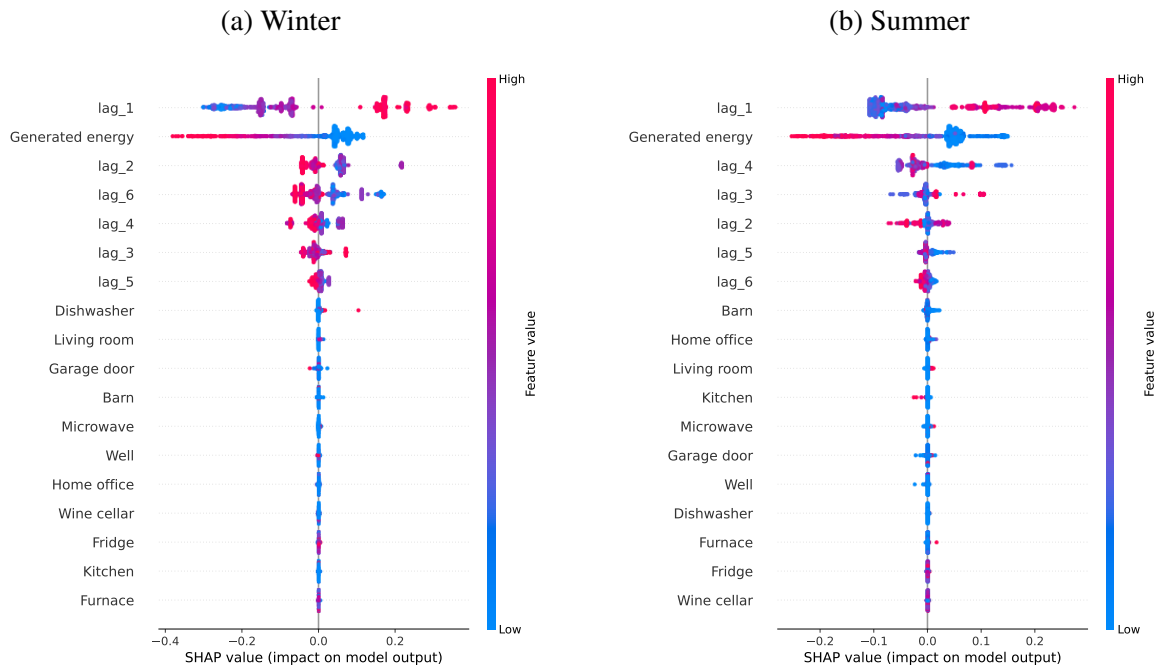


Figure 5 Time series’ appliances impact into net baseload demand IO estimates via SHAP values

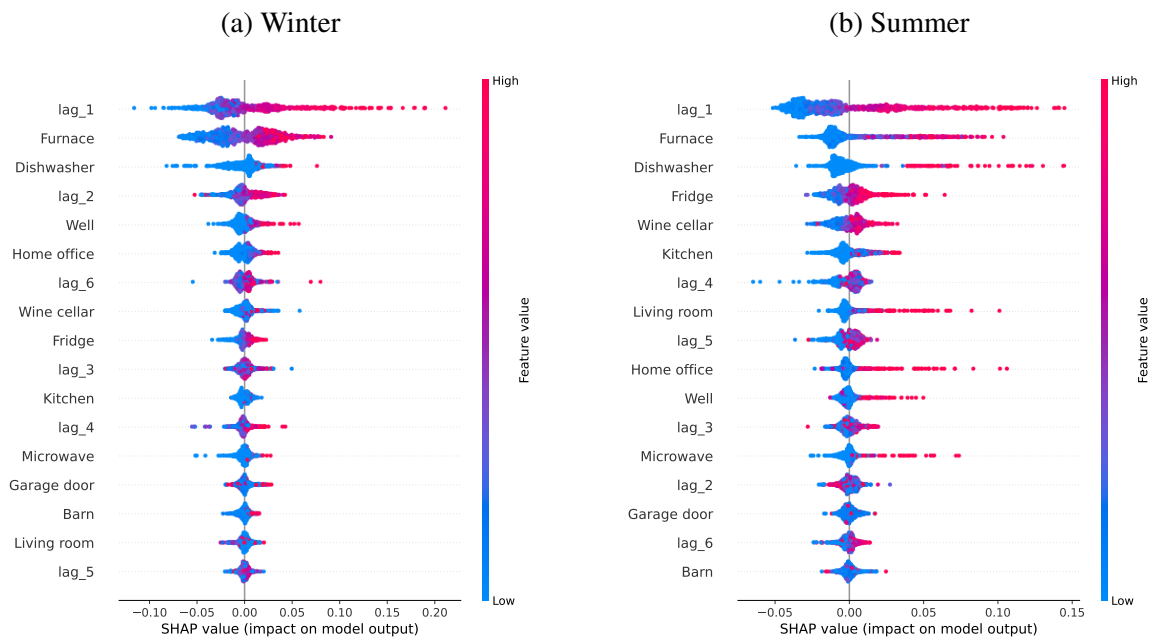


Figure 6 Time series’ appliances impact into flexible IO estimates via SHAP values

Thus, in concluding this section, we observe that, with confidence in the approach, we can now turn to the second set of consumer response data where there is a well defined TOU tariff, but the details of their responses are unobserved. This is the more realistic setting which motivated the research.

Table 6 Error metrics

	IO		XGboost		SARIMA		SARIMAX	
	MAE	RMSE	MAE	RMSE	MAE	RMSE	MAE	RMSE
C137	0.0179	0.0224	0.0272	0.0329	0.0190	0.0230	0.0217	0.0260
C162	0.0449	0.0608	0.0544	0.0740	0.0457	0.0609	0.0540	0.0653

Table 7 Error metrics for the net load probabilistic forecasting for the conscious demand-response program Quantiles and CRPS

	IO			XGboost			SARIMA			SARIMAX		
	$q_{0.05}$	$q_{0.95}$	CRPS	$q_{0.05}$	$q_{0.95}$	CRPS	$q_{0.05}$	$q_{0.95}$	CRPS	$q_{0.05}$	$q_{0.95}$	CRPS
C137	0.046	0.090	0.018	0.047	0.118	0.021	0.037	0.131	0.016	0.036	0.133	0.017
C162	0.125	0.235	0.038	0.118	0.302	0.038	0.131	0.283	0.042	0.132	0.287	0.043

5.2 Predictability with estimated price responsive components

This example is more common in practice when the SO sets the TOU electricity tariffs and observes the net load of the consumer at its meter, but, for privacy or agency reasons, it cannot observe the actual customer's appliance behavior. The dataset is taken from a Japanese utility as reported by [Kiguchi et al. \(2021\)](#). We consider the weekdays corresponding to the period from July to September 2018 and the goal is to predict the last week of September. Exogenous weather variables are the scaled sine and cosine temperatures and ground solar irradiance values at Tokyo. We selected two customers, being the customers 137 and 162 available by [Kiguchi et al. \(2021\)](#). For p_t in the IO model the flat tariff was 26JPY/kWh and we defined $p_t^{sf,+} = \max(p_t - \text{TOU}_t, 0)$, $p_t^{sf,-} = \max(\text{TOU}_t - p_t, 0)$, where $\text{TOU}_t = 35$ JPY/kWh between 2pm and 10pm, and 20JPY/kWh otherwise. The parameters for load shedding are defined by $\sum_{t \in [T]} p_t^{sf,+} / 24$. The parameters $c_t^{sf,+}$, $c_t^{sf,-}$ are set to $|p_t - \text{TOU}_t|$ when $p_t^{sf,+}$, $p_t^{sf,-}$ are equal to zero, respectively, and 0, otherwise.

Figures 8 and 9 show the time series of the load components estimated by the IO method for customers 137 and 162. As before with the Kaggle data, the peak price time periods are highlighted in pink in the figures. Again it is reassuring to see that the demand drops during the peak prices in the flexible load profiles but not in the baseload, and that demand shifting is evident with the flexible loads increasing at the end of hose periods. The baseload components are very regular in their periodicities. The ability to identify these series from the unobserved consumer demand responses is the most remarkable aspect of this methodology. From the previous results, we also expect greater forecasting accuracy as a consequence.

Thus, Table 6 shows the performance metrics for the four methods under consideration. It is evident that the IO approach yields better point forecasts than the other methods. Additionally, it is noted that XGboost, despite being a favored technique for accuracy, demonstrates an inclination towards overestimation and significant fluctuations in the point load forecasts. To be more precise, for customer C137, XGBoost shows

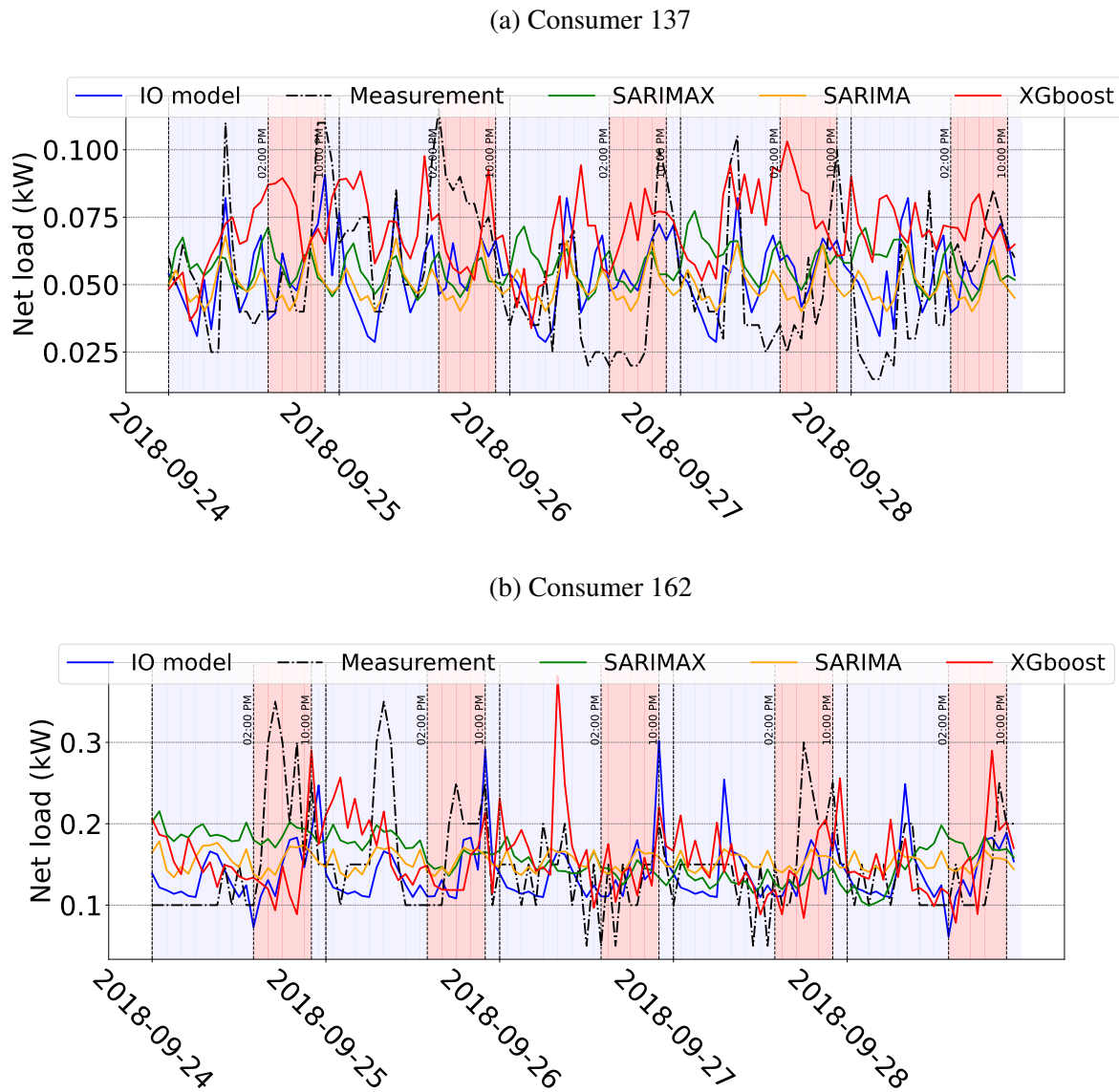


Figure 7 Net Load profiles and performance error metrics under best hyperparameter tuning for the conscious demand-response program case study

approximately 52% higher MAE and 47% higher RMSE compared to IO method. SARIMA exhibits about 6% higher MAE and 3% higher RMSE, while SARIMAX shows approximately 21% higher MAE and 16% higher RMSE than IO method. Similarly, for customer C162, XGBoost demonstrates around 21% higher MAE and 22% higher RMSE, SARIMA shows about 2% higher MAE and 0.2% higher RMSE, and SARIMAX exhibits approximately 20% higher MAE and 7% higher RMSE compared to IO method.

As with the previous study, a probabilistic forecasting analysis was also conducted to assess the quality of density forecasting. The data in Table 7 shows the quantiles and CRPS (averaged over the forecasting horizon). XGBoost consistently reports higher errors across metrics for both customers. For Customer C137, XGBoost has quantile errors with $q_{0.05}$ 2.2% higher and $q_{0.95}$ 31.1% higher compared to IO. SARIMA and

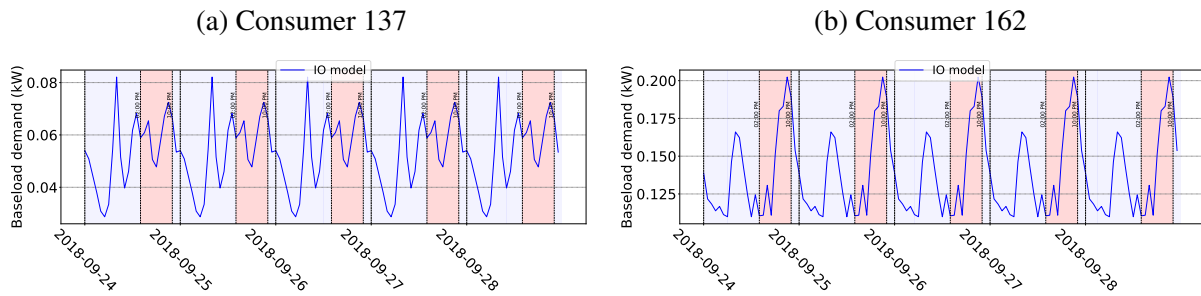


Figure 8 Baseload demand profile estimates

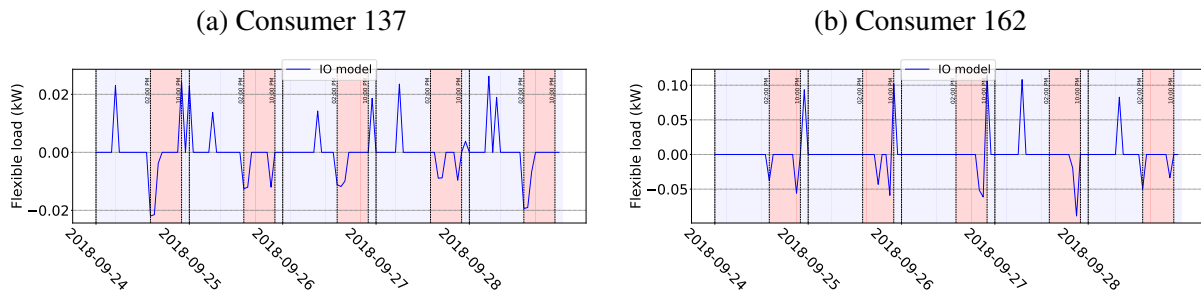


Figure 9 Flexible Load profile estimates

SARIMAX perform similarly to IO in quantile estimation and slightly better in CRPS for this specific customer, C137. Regarding Customer C162, XGBoost exhibits quantile errors 5.6% higher for $q_{0.05}$ and 32.5% higher for $q_{0.95}$. compared to IO, with SARIMA and SARIMAX again demonstrating comparable performance to IO in quantile’s estimation and CRPS but a little worse for this customer in CRPS.

In summary, while XGBoost consistently delivers higher errors across deterministic and probabilistic metrics, the IO method proves to be more accurate in load forecasting and uncertainty quantification. SARIMA performs similarly to IO in probabilistic forecasting goals and a slightly better than SARIMAX. However, IO delivers a better interpretability of demand flexibility while SARIMA just captures some autoregressive and seasonal behavior during the summer period. Thus, in the more realistic setting provided by this dataset, the IO approach appears to be more accurate and more transparent in its revelations of the unobserved components.

6 Conclusions

In this paper, we have addressed an emerging information management challenge in retail electricity. Accurately characterizing the components of consumer electricity demand response is critical for system operators and energy retailers, but achieving this requires usually real-time, device-level data. However, such data is often unavailable or restricted due to data protection policies. Instead, all that can be observed is the net demand at the meters connecting customers to the grid, whilst the “behind-the-meter” demand components remain unobservable. As a result, alternative methods which can infer or impute this unobservable

information have substantial value. Current approaches fall short in this regard. To tackle this challenge, we developed and tested a data-driven inverse optimization (IO) methodology that effectively addresses this methodological gap.

Unlike conventional methods, the IO approach does not depend on direct observation of device-level data or behind-the-meter activities. Instead, it utilizes net demand data to estimate parameters within a latent optimization model, enabling the decomposition of consumption patterns into both observable and unobservable components. This includes net demand influenced by consumer behavior, as well as underlying baseload and flexible elements, such as shifted and sheddable loads. The inverse optimization (IO) methodology effectively captures the nonlinear relationships between price responses and external factors, providing a more nuanced and accurate understanding of consumer electricity demand response.

Having developed a solution methodology for the specific IO formulation, we conducted a comprehensive experimental study to assess the outcome in two different settings. In the first setting, we evaluated the empirical efficacy of the proposed IO methodology against established benchmarks by assessing of the construct validity of the identified flexible and baseload components. By regressing the estimated activities of these components on the known usage patterns of household appliances and autoregressive lags, we showed that discretionary appliance usage is prevalent in the flexible component, while autoregressive influences are more prominent in the baseload component, reflecting adaptive and habitual behaviors. In the second setting, through a precise TOU responses of consumer data from Japan, we showed that the price response of domestic customers can be more accurately estimated using an IO decomposition of flexible and baseload components compared to conventional benchmark methods. This finding supports the proposition that IO can be practically useful compared to traditional forecasting methods without jeopardizing interpretability and forecast accuracy.

This research contributes to the objectives of Green IS by providing system operators, retailers and regulators with a new practical approach to deal with the growing complexity of electricity consumption by end-users in the energy transition. The method enables system operators and retailers to gain a deeper understanding of behind-the-meter flexibility which might otherwise be precluded by data privacy and restricted access to real-time device-level measurements. Crucially, this approach leads to more accurate consumer demand forecasts compared to conventional benchmarks. By accurately characterizing demand components, this approach could enhance grid operations, improve revenue management for retailers, and facilitate more efficient pricing. Further applications will be needed to establish real benefits, but this research has demonstrated its potential.

References

Amat Rodrigo, Joaquin, Javier Escobar Ortiz. 2024. skforecast. doi:10.5281/zenodo.8382788. URL <https://skforecast.org/>.

- An, Jaeyong, PR Kumar, Le Xie. 2015. On transfer function modeling of price responsive demand: An empirical study. *2015 IEEE power & energy society general meeting*. IEEE, 1-5.
- An, Jaeyong, PR Kumar, Le Xie. 2016. Dynamic modeling of price responsive demand in real-time electricity market: Empirical analysis. *arXiv preprint arXiv:1612.05021*, .
- Aswani, Anil, Zuo-Jun Shen, Auyon Siddiq. 2018. Inverse optimization with noisy data. *Operations Research*, 66 (3), 870-892.
- Bian, Yuexin, Ningkun Zheng, Yang Zheng, Bolun Xu, Yuanyuan Shi. 2022. Demand response model identification and behavior forecast with optnet: a gradient-based approach. *Proceedings of the Thirteenth ACM International Conference on Future Energy Systems*. e-Energy '22, Association for Computing Machinery, New York, NY, USA, 418–429. doi:10.1145/3538637.3538871. URL <https://doi.org/10.1145/3538637.3538871>.
- Bian, Yuexin, Ningkun Zheng, Yang Zheng, Bolun Xu, Yuanyuan Shi. 2023. Predicting strategic energy storage behaviors. *arXiv preprint arXiv:2306.11872*, .
- Bynum, Michael L., Gabriel A. Hackebeil, William E. Hart, Carl D. Laird, Bethany L. Nicholson, John D. Siirola, Jean-Paul Watson, David L. Woodruff. 2021. *Pyomo—optimization modeling in python*, vol. 67. 3rd ed. Springer Science & Business Media.
- Cappers, Peter, Charles Goldman, David Kathan. 2010. Demand response in US electricity markets: Empirical evidence. *Energy*, 35 (4), 1526-1535.
- Chan, Timothy CY, Rafid Mahmood, Ian Yihang Zhu. 2023. Inverse optimization: Theory and applications. *Operations Research*, .
- Chen, Liudong, Xiangqi Zhu, Bolun Xu, Fei Ding. 2024. Demand side flexibility envelope quantification under data scarcity. *2024 IEEE Power & Energy Society Innovative Smart Grid Technologies Conference (ISGT)*. IEEE, 1-5.
- Chen, Tianqi, Carlos Guestrin. 2016. Xgboost: A scalable tree boosting system. *Proceedings of the 22nd acm sigkdd international conference on knowledge discovery and data mining*. 785-794.
- Choi, Dong Gu, Michael K Lim, Karthik Murali, Valerie M Thomas. 2020. Why have voluntary time-of-use tariffs fallen short in the residential sector? *Production and Operations Management*, 29 (3), 617-642.
- Danti, Piero, Sandro Magnani. 2017. Effects of the load forecasts mismatch on the optimized schedule of a real small-size smart prosumer. *Energy Procedia*, 126 406-413.
- Dobakhshari, Donya Ghavidel, Vijay Gupta. 2018. A contract design approach for phantom demand response. *IEEE Transactions on Automatic Control*, 64 (5), 1974-1988.
- Dong, Ciwei, Chi To Ng, TCE Cheng. 2017. Electricity time-of-use tariff with stochastic demand. *Production and operations management*, 26 (1), 64-79.
- European Parliament and Council. 2016. Regulation (eu) 2016/679 of the european parliament and of the council. Official Journal of the European Union. URL <https://eur-lex.europa.eu/legal-content/EN/TXT/?uri=CELEX%3A02016R0679-20160504>. Accessed: 2024-07-29.

- Fernández-Blanco, Ricardo, Juan Miguel Morales, Salvador Pineda. 2021a. Forecasting the price-response of a pool of buildings via homothetic inverse optimization. *Applied Energy*, 290 116791.
- Fernández-Blanco, Ricardo, Juan Miguel Morales, Salvador Pineda, Álvaro Porras. 2021b. Inverse optimization with Kernel regression: Application to the power forecasting and bidding of a fleet of electric vehicles. *Computers & Operations Research*, 134 105405.
- Gneiting, Tilmann, Roopesh Ranjan. 2011. Comparing density forecasts using threshold- and quantile-weighted scoring rules. *Journal of Business & Economic Statistics*, 29 (3), 411-422. doi:10.1198/jbes.2010.08110.
- Hatton, Leslie, Philippe Charpentier, Eric Matzner-Løber. 2015. Statistical estimation of the residential baseline. *IEEE Transactions on Power Systems*, 31 (3), 1752-1759.
- Hekmat, Nami, Hanmin Cai, Thierry Zufferey, Gabriela Hug, Philipp Heer. 2023. Data-driven demand-side flexibility quantification: Prediction and approximation of flexibility envelopes. *2023 IEEE Belgrade PowerTech*. IEEE, 1-6.
- Karthikeyan, S Prabhakar, I Jacob Raglend, Dwarkadas P Kothari. 2013. A review on market power in deregulated electricity market. *International Journal of Electrical Power & Energy Systems*, 48 139-147.
- Kiguchi, Y, M Weeks, R Arakawa. 2021. Predicting winners and losers under time-of-use tariffs using smart meter data. *Energy*, 236 121438.
- Kirschen, Daniel S, Goran Strbac, Pariya Cumperayot, Dilemar de Paiva Mendes. 2000. Factoring the elasticity of demand in electricity prices. *IEEE Transactions on Power Systems*, 15 (2), 612-617.
- Kleinert, Thomas, Martin Schmidt. 2023. Why there is no need to use a big-m in linear bilevel optimization: A computational study of two ready-to-use approaches. *Computational Management Science*, 20 (1), 3.
- Koliou, Elta, Cajsa Bartusch, Angela Picciariello, Tobias Eklund, Lennart Söder, Rudi A Hakvoort. 2015. Quantifying distribution-system operators' economic incentives to promote residential demand response. *Utilities Policy*, 35 28-40.
- Kovács, András. 2021. Inverse optimization approach to the identification of electricity consumer models. *Central European Journal of Operations Research*, 29 (2), 521-537.
- Lei, Shunbo, David Hong, Johanna L Mathieu, Ian A Hiskens. 2020. Baseline estimation of commercial building HVAC fan power using tensor completion. *Electric Power Systems Research*, 189 106624.
- Lin, Jun, Jin Ma, Jianguo Zhu. 2021. A privacy-preserving federated learning method for probabilistic community-level behind-the-meter solar generation disaggregation. *IEEE Transactions on Smart Grid*, 13 (1), 268-279.
- Liu, Jing, Yang Xiao, Shuhui Li, Wei Liang, CL Philip Chen. 2012. Cyber security and privacy issues in smart grids. *IEEE Communications surveys & tutorials*, 14 (4), 981-997.
- Loock, Claire-Michelle, Thorsten Staake, Frédéric Thiesse. 2013. Motivating energy-efficient behavior with green is: an investigation of goal setting and the role of defaults. *MIS quarterly*, 1313-1332.
- Lu, Tianguang, Zhaoyu Wang, Jianhui Wang, Qian Ai, Chong Wang. 2018. A data-driven stackelberg market strategy for demand response-enabled distribution systems. *IEEE Transactions on Smart Grid*, 10 (3), 2345-2357.

- Mahdavi, Nariman, Dilusha Weeraddana, Ying Guo. 2022. Probabilistic estimation of pv generation at customer and distribution feeder levels using net-demand data. *IEEE Transactions on Smart Grid*, 14 (3), 1974-1984.
- Mohajerin Esfahani, Peyman, Soroosh Shafieezadeh-Abadeh, Grani A Hanasusanto, Daniel Kuhn. 2018. Data-driven inverse optimization with imperfect information. *Mathematical Programming*, 167 191-234.
- MOSEK. 2024. *MOSEK ApS*. URL <https://www.mosek.com>.
- Nghiem, Truong X, Colin N Jones. 2017. Data-driven demand response modeling and control of buildings with gaussian processes. *2017 American Control Conference (ACC)*. IEEE, 2919-2924.
- Pinson, Pierre, Henrik Madsen, et al. 2014. Benefits and challenges of electrical demand response: A critical review. *Renewable and Sustainable Energy Reviews*, 39 686-699.
- Ponoćko, Jelena, Jovica V Milanović. 2018. Forecasting demand flexibility of aggregated residential load using smart meter data. *IEEE Transactions on Power Systems*, 33 (5), 5446-5455.
- Ruan, Guangchun, Daniel S Kirschen, Haiwang Zhong, Qing Xia, Chongqing Kang. 2021. Estimating demand flexibility using siamese lstm neural networks. *IEEE Transactions on Power Systems*, 37 (3), 2360-2370.
- Saez-Gallego, Javier, Juan M Morales. 2017. Short-term forecasting of price-responsive loads using inverse optimization. *IEEE Transactions on Smart Grid*, 9 (5), 4805-4814.
- Saez-Gallego, Javier, Juan M. Morales, Marco Zugno, Henrik Madsen. 2016. A data-driven bidding model for a cluster of price-responsive consumers of electricity. *IEEE Transactions on Power Systems*, 31 (6), 5001-5011. doi:10.1109/TPWRS.2016.2530843.
- Shahidehpour, Mohammad, Hatim Yamin, Zuyi Li. 2002. *Market operations in electric power systems: forecasting, scheduling, and risk management*. John Wiley & Sons.
- Shi, Yuanyuan, Bolun Xu. 2023. Demand-side price-responsive flexibility and baseline estimation through end-to-end learning. *IET Renewable Power Generation*, .
- Siddiqui, Sauleh, Steven A Gabriel. 2013. An sos1-based approach for solving mpecs with a natural gas market application. *Networks and Spatial Economics*, 13 205-227.
- Singh, T. 2024. Smart home dataset with weather information [online], Available at: URL <https://www.kaggle.com/taranvee/smart-home-dataset-with-weather-information>.
- Srivastava, Ankur, Junbo Zhao, Hao Zhu, Fei Ding, Shunbo Lei, Ioannis Zografopoulos, Rabab Haider, Soroush Vahedi, Wenyu Wang, Gustavo Valverde, et al. 2024. Distribution system behind-the-meter ders: Estimation, uncertainty quantification, and control. *IEEE Transactions on Power Systems*, .
- Sun, Mingyang, Yi Wang, Fei Teng, Yujian Ye, Goran Strbac, Chongqing Kang. 2019. Clustering-based residential baseline estimation: A probabilistic perspective. *IEEE Transactions on Smart Grid*, 10 (6), 6014-6028.
- Sunar, Nur, Jayashankar M Swaminathan. 2022. Socially relevant and inclusive operations management. *Production and Operations Management*, 31 (12), 4379-4392.
- Tlenshiyeva, Akmaral, Marcos Tostado-Véliz, Hany M Hasanien, Nima Khosravi, Francisco Jurado. 2024. A data-driven methodology to design user-friendly tariffs in energy communities. *Electric Power Systems Research*,

228 110108.

- Vallés, Mercedes, Antonio Bello, Javier Reneses, Pablo Frías. 2018. Probabilistic characterization of electricity consumer responsiveness to economic incentives. *Applied Energy*, 216 296-310.
- Vardakas, John S, Nizar Zorba, Christos V Verikoukis. 2014. A survey on demand response programs in smart grids: Pricing methods and optimization algorithms. *IEEE Communications Surveys & Tutorials*, 17 (1), 152-178.
- Watson, Richard T, Marie-Claude Boudreau, Adela J Chen. 2010. Information systems and environmentally sustainable development: energy informatics and new directions for the is community. *MIS quarterly*, 23-38.
- Wen, Lulu, Kaile Zhou, Jun Li, Shanyong Wang. 2020. Modified deep learning and reinforcement learning for an incentive-based demand response model. *Energy*, 205 118019.
- Zhang, Xiao-Yu, Chris Watkins, Stefanie Kuenzel. 2022. Multi-quantile recurrent neural network for feeder-level probabilistic energy disaggregation considering roof-top solar energy. *Engineering Applications of Artificial Intelligence*, 110 104707.
- Zhang, Yi, Weiwei Chen, Rui Xu, Jason Black. 2015. A cluster-based method for calculating baselines for residential loads. *IEEE Transactions on smart grid*, 7 (5), 2368-2377.
- Zhou, Bo, Ruiwei Jiang, Siqian Shen. 2024. Learning to solve bilevel programs with binary tender. *Conference paper at ICLR 2024*, .